Meteorologica

**Artículo en edición**

# THE RIO DE LA PLATA ESTUARY HYDROLOGY AND CIRCULATION

**Diego Moreira and Claudia Simionato**

**Departamento de Ciencias de la Atmósfera y los Océanos (DCAO, FCEN-UBA), Centro de Investigaciones del Mar y la Atmósfera (CIMA, CONICET-UBA) and Instituto Franco-Argentino para el Estudio del Clima y sus Impactos (UMI IFAECI, CNRS-CONICET-UBA). Ciudad Universitaria, Pabellón II Piso 2 (C1428EHA) Ciudad Autónoma de Buenos Aires, Argentina**

**Autor correspondiente: Diego Moreira,** moreira@cima.fcen.uba.ar

Manuscrito recibido el 29 de agosto de 2017; Manuscrito aceptado el 1 de diciembre de 2017

## RESUMEN

Este trabajo compila y resume los conocimientos actuales sobre la hidrología y circulación del Estuario del Río de la Plata, revisando la literatura existente sobre el tema. En primer lugar, se describen los principales forzantes de la circulación en el estuario -su geometría y batimetría, descarga, olas, mareas y vientos- enfatizando, cuando corresponde, en sus escalas temporales de variabilidad de intra a inter-anual. Luego, se discuten la estructura de la densidad y los principales patrones de circulación, sintetizando los resultados obtenidos a partir de estudios basados en modelos y en observaciones. La descripción de la circulación se realiza en dos partes: (i) en primer lugar, se presenta la circulación barotrópica (media vertical) con gran impacto en el transporte neto de masa y, por lo tanto, en la variabilidad del nivel del agua en el estuario, (ii) en segundo lugar, se discute lo que se conoce acerca de las corrientes baroclínicas (que varían verticalmente) en la zona frontal y su influencia en la estructura de densidad. Finalmente, se describen los caminos de las masas de agua dulce de los principales afluentes a lo largo del estuario y se discuten los mecanismos que favorecen la retención en la zona frontal.

**Palabras clave:** Estuario del Río de la Plata, hidrodinámica, circulación, escalas de mezcla

## ABSTRACT

This work compiles and summarizes the current knowledge of the Río de la Plata Estuary hydrology and circulation, reviewing the existing literature on the issue. We firstly describe the main forcings of the circulation in the estuary -its geometry and bathymetry, runoff, wind-waves, tides and winds- emphasizing, when it applies, in their temporal scales of variability from intra to inter-annual. Then, we discuss the density structure and the main circulation patterns, synthesizing results derived from modelling and observational studies. The description of the circulation is done in two parts: (i) firstly reporting the barotropic (vertically averaged) motion, which strongly affects the net mass transport and sea surface height variability in the estuary and, therefore, is linked to the surges; and (ii) secondly, discussing what it is known about the baroclinic (vertically varying) currents in the frontal zone and their influence on the density structure. Finally, the paths of the freshwater masses of the main tributaries along the estuary are described and the mechanisms that favour retention in the frontal zone are discussed.

Artículo en edición

**Keywords**: Río de la Plata Estuary, hydrodynamics, circulation, flushing scales

## Introduction

It has been estimated that 23% of the world population ($1.2 \times 10^9$ people) lives near the coasts (less than 100 km and up to 100 m above sea level), while the density of the population in these coastal regions is three times larger than the global average (Small and Nicholls, 2003). One of these densely populated sites is located in the Río de la Plata (RdP) Estuary, the most developed area of Southern South America, located at 35 ºS on the south-western South Atlantic.

The RdP (Figure 1) has large social and economic importance for the countries along its shores, Argentina and Uruguay. It drains the second largest basin of South America, formed by the Paraná and the Uruguay rivers. The estuarine area is 35,000 $km^2$ and the fluvial drainage area is $3.1\times10^6$ $km^2$ (Depetris and Griffin, 1968), which ranks the RdP in fourth and fifth in the world in fluvial discharge and drainage area, respectively. The capital cities of both countries, Buenos Aires and Montevideo, and a number of harbours, resorts and industrial centres are located on its margins and influence zone. This estuary is the main source of drinking water for millions of inhabitants in the hinterlands, for whom it is also an important amusement area. The RdP constitutes the access to the most important harbours of southern South America, including those of Argentina and Uruguay; the navigation channels of these ports demands a continuous dredging. In addition, the transfers of commodities to Paraguay from and to overseas countries is also made though the estuary and its tributary rivers. The estuary contains one of the largest wetlands of the region in Samborombón Bay, which is the home for a number of species of fishes, turtles, crabs and migratory birds (Lasta, 1995; Canevari *et al.,* 1998; Volpedo *et al.,* 2005).

The drainage of rich in organic detritus and nutrients freshwater enriches the estuary and provides highly productive habitats for a large number of organisms. The convergence of fresh and salt water generates a border system (an ecotone) that favours spawning and nursery for several coastal species (*e.g.,* Acha and Macchi, 2000; Berasategui *et al.,* 2004; Rodrigues, 2005; Berasategui *et al.*, 2006; Acha *et al.,* 2008; Derisio *et al.*, 2014). All these aspects are highly conditioned by the variability in the salinity and the sedimentology which, in turn, is mostly governed by the circulation (*e.g.*, Simionato *et al*., 2007; Meccia *et al*., 2013; Moreira, 2016).

In what regards the impact on the adjacent ocean, the fresh water plume of the RdP influences the shelf over a distance of more than 500 km to the north (Campos *et al.,* 1999), exporting water, sediments, carbon and nutrients. Using the first remote observations of Sea Surface Salinity coming from Aquarius and SMOS, Guerrero *et al.* (2014) show how the Río de la Plata waters are exported towards the deep ocean in the region of Brazil-Malvinas Confluence. Consequently, this estuary has an obvious impact on the adjacent shelf and the boundary currents system (*e.g*., Machado *et al.*, 2013; Combes and Matano, 2014).

Many environmental questions in the RdP and the adjacent shelf are linked to the circulation, its variability and its principal forcings. Some of the most significant issues include drinking water resources, storm surges forecast (*e.g.*, Dinápoli *et al*., 2017), floods alerts (*e.g.*, Moreira *et al.*, 2014), waste drainage, optimization of dredging operations (*e.g*., Cardini *et al.,* 2002), understanding geomorphological change (*e.g*., Codignotto *et al.,* 2011; Cellone *et al*., 2016), contamination (*e.g*., Colombo *et al.,* 2005; 2007; Avigliano *et al.,* 2015), benthic ecology (*e.g*., Gómez-Erache, 1999), primary productivity (*e.g*., Gómez-Erache *et al.,* 2004; Huret *et al.,* 2005) and fisheries (*e.g*., Jaureguizar *et al.,* 2003a,b; Acha *et al.,* 2008; Jaureguizar *et al.,* 2008; 2016).

The water circulation in the RdP Estuary and in the adjacent shelf is driven by the complex interaction of several forcings (drivers) -the tributaries flow, the tides, the winds, the geometry and the bottom topography- and is affected by the rotation of the Earth. The high variability of the winds in the area and the large breadth of the estuary give to circulation particular features (*e.g*. Simionato *et al*., 2004a,b; 2006a,b; Meccia *et al.*, 2009; 2013).

Given the large impact of the RdP circulation on a number of scientific questions so as in management, the aim of this work is to compile, summarize and integrate most of the numerous papers that have been produce regarding the estuary circulation and hydrology. We hope that this work will facilitate the access to the information to a broad audience, particularly to those who are not specialized in physical processes in estuaries.

## 1. Geographic setting and forcings

### 2.1. Main bathymetric features

An estuary can be defined as an embayment of the coast in which buoyancy forcing alters the fluid density from that of the adjoining ocean (Valle-Levinson, 2010; Geyer and MacCready, 2014). The RdP estuary (Figure 1), in particular, is one of the largest estuaries in the world (Shiklomanov, 1998). It is located on the eastern coast of southern South America at approximately 35ºS, and has a northwest to southeast oriented funnel shape approximately 320 km long, which narrows from 230 km at its mouth to 40 km at its upper end (Balay, 1961). A complete description of its morphology and sedimentology can be found in Ottman and Urien (1966), Depetris and Griffin (1968), Urien (1972), Parker *et al.* (1986), López Laborde (1987), Moreira *et al.* (2016), and references therein. Based on its morphology and on what is known or inferred about its dynamics, the RdP Estuary has been classically divided into two regions split by the Barra del Indio, a submerged shoal with a slightly convex shape and depths of 6.5-7 m which crosses the estuary between

Punta Piedras and Montevideo. The upper region is almost occupied by freshwater and is characterized by shallow banks with depths ranging from 1 to 4 m (Playa Honda and Ortiz Bank), which are separated from the coasts by deeper channels with depths varying from 5 to 8 m (North, Oriental and Intermediate Channels) and limited to the south by the Barra del Indio. Eastwards the shoal, the Maritime Channel, a wide depression with depth increasing from 12 to 14 m at the north to 20 m at the south, separates Samborombón Bay to the west from a region of banks known as Alto Marítimo to the east. The Alto Marítimo is formed by the Arquímedes and English Banks, with depths ranging from 6 to 8 m, and the Rouen Bank with a depth of 10-12 m. To the north of those banks, the Oriental Channel, the deepest channel of the estuary with depths of up to 25 m, extends along the Uruguayan coast. Samborombón Bay is a very shallow and extensive area with depths ranging from 2 to 10 m that extends between Punta Piedras to the north and Punta Rasa to the south.

### 2.2. The continental discharge

Freshwater reaches the RdP Estuary through a number of tributaries (Figure 2), being the two major the Paraná and Uruguay rivers. Those rivers form the second largest basin of South America after the Amazon, with a mean discharge for the 1931-2016 period of 23,000 $m^3s^{-1}$ (Borús and Giacosa, 2014; Borús *et al*., 2017). The Paraná River flows into the estuary forming a large delta; the two main branches are the Paraná Guazú-Bravo, transporting approximately 77% of the runoff, and the Paraná de las Palmas, transporting the remaining 23% (Nagy *et al.*, 1997; Jaime and Menéndez, 2002). The mean transport of the minor tributaries is several orders of magnitude less and, therefore, the average continental discharge to the estuary can be almost evaluated as the result of the transport of the two major tributaries (Framiñan *et al.,* 1999).

The RdP flow regime showed large inter-annual and inter-decadal variability. On inter-decadal time scales a normal runoff cycle, that spanned between 1931 and 1943, a dry period during 1944-1970 and humid period starting in 1971 were reported (Jaime and Menéndez, 2002). The increment of the mean flow from the dry to the humid phase reported by Jaime and Menéndez (2002) was significant: 15% more than the historical mean and 33% more than the 1944-1970 mean. The mean runoff from 1971 to 2002 rose to 24,000 $m^3s^{-1}$ (Jaime and Menéndez, 2002) and to 25,000 $m^3s^{-1}$ between 1997 and 2016 (Borús *et al.*, 2017).

The runoff variability in inter-annual time scale has been studied by Mechoso and Perez-Iribarren (1992), Robertson and Mechoso (1998), Jaime and Menéndez (2002; 2003). It displays a near-decadal component, and inter-annual peaks at El Niño - Southern Oscillation (ENSO) timescales. The near-decadal component, in which high river runoff is associated with anomalously cool sea surface temperatures (SST) over the tropical North Atlantic, is most marked in the Paraná River. Instead, ENSO timescale variability (with peaks at bands centred at about 2.5 and 3.5 years) is more pronounced in the Uruguay River, with El Niño (La Niña) associated with enhanced (reduced) stream flow. Additionally, another peak of variability centred at 6.5 years has been recorded for this river. It is related to a pattern of large SST anomalies in the central and western Pacific, with large off-equatorial anomalies farther east. This spatial pattern is characteristic of longer timescale variability over the tropical Pacific. Over the South Atlantic, the SSTs associated to this cycle resemble the semi-quadrennial one. However, the SST anomaly pattern over the tropical North Atlantic is of the opposite sign, with cold anomalies accompanying positive stream-flow anomalies. Peaks as large as 90,000 $m^3s^{-1}$ and as low as 8,000 $m^3s^{-1}$ have been recorded in association with those cycles.

The total discharge to the RdP Estuary displays a weak seasonality; this is because of the weak seasonality of the tributaries, and the fact that their cycles are out of phase, partially compensating each other (Nagy *et al.,* 1997). The mean seasonal cycle of the main tributaries and of the total runoff to the RdP is shown in Figure 3. The Paraná Guazú river displays a maximum runoff between March and June and a minimum in October (Figure 3, green line). The Paraná de las Palmas (blue line), with a lower runoff, has a maximum between March and May and a minimum in October. The Uruguay River displays two maxima, one in October-November and the other in May-June, and a minimum in January. This way, the total runoff is around 30,000 $m^3s^{-1}$ in winter and around 23,000 $m^3s^{-1}$ in summer.

Meccia *et al.* (2009) and Saraceno *et al.* (2014) showed from numerical simulations and satellite observations that the runoff that reaches the RdP Estuary is the main modulator of the inter-annual time scale variability of the sea surface height (SSH). They estimated that the changes in the mean sea level associated to the extreme discharge conditions might vary from ±0.25 m at the uppermost RdP (Meccia *et al.,* 2009), to the order of ±0.03 m at the exterior estuary. The variability on inter-annual time scales of the continental discharge has a strong impact on the position of the surface and bottom salinity fronts of the RdP (FREPLATA, 2005; Guerrero *et al*., 2010), the turbidity (Dogliotti *et al*., 2016), the retention properties at the estuary (Acha *et al.*, 2012), the grow of marshes (Schuerch *et al.*, 2016), the chlorophyll-a concentration(Machado *et al.*, 2013)and the structure of the phytoplankton, with a significant reduction of diversity and decreases in biomass and phytoplankton density, during El Niño phases (Satchiq *et al.*, 2015). Also, it has been reported that cyanobacteria are more abundant in the neutral periods, Chlorophyceae dominate during La Niña phase and Bacyllariophyceae dominate during El Niño (Satchiq *et al*., 2015). Finally, the warm-phase ENSO events increase the trophic state of the sediments because of the increased freshwater input (García-Rodriguez *et al*., 2014). The variability on seasonal time scale of the runoff has a large impact on turbidity (*e.g.*, Moreira *et al.*, 2013) and a low impact on sea level (Meccia *et al.*, 2009).

### 2.3. Tides

The RdP is a microtidal system and the tidal regime is mixed, dominantly semidiurnal. The principal lunar semi-diurnal $M_2$ is the most significant constituent ($M_2$ has an amplitude of 0.27 m at Buenos Aires and around 0.65 m in Samborombón Bay, Figure 4 upper panel, Simionato *et al.*, 2004a); however, there are significant diurnal inequalities, mostly caused by the principal lunar diurnal constituent $O_1$, with an amplitude of 0.15 m at Buenos Aires (D'Onofrio *et al.,* 1999). This way, maximum amplitude at Buenos Aires (upper estuary) can reach 1 m, whereas the mean is 0.6 m. At Punta Rasa, the maximum amplitude reaches 1.43 m and the mean is of 0.76 m (SHN, 2017).

Tidal waves associated with the South Atlantic amphidromes reach the Continental Shelf while propagating northward (O'Connor 1991; Glorioso and Flather 1995, 1997; Simionato *et al.,* 2004a). As they propagate over the shelf, geographic setting modifies their propagation so that energy enters the estuary mainly from the southeast (Simionato *et al.,* 2004a). The tide (Figure 4 upper left panel) propagates as a Kelvin wave forced at the estuary mouth, leaving the coast to the left in the Southern Hemisphere; therefore, tidal amplitudes are larger and currents are stronger along the Argentinean coast than along the Uruguayan one (Simionato *et al.,* 2004a). The tide propagates at the phase speed ($c$) of long external gravity waves $c=\lambda/T=\sqrt{gH}$, where $\lambda$ is the wavelength, $T$ is the period, $g$ is the acceleration of gravity and $H$ is the depth. In consequence, as the wave progresses towards the estuary head, $H$ decreases and therefore, c and λ must decrease. Owing to this effect and the considerable length of the estuary, semidiurnal constituents have the unusual feature of nearly complete a wavelength within the estuary at all times (CARP, 1989). Tidal amplitudes are generally not amplified toward the upper part (Figure 4). The estuary is long and converges only at its innermost part, where it is extremely shallow and bottom friction plays a fundamental role controlling the wave amplitude (Framiñan *et al.,* 1999). This way, dissipation by bottom friction is large, and most of the energy is lost before the tidal wave reaches the upper estuary (Figure 4 lower panel); as a consequence, tides have small amplitude in the upper estuary and along its northern coast (Simionato *et al.,* 2004a).

Given that water level is easier to measure than tidal currents, observations of this last variable are scarcer, and much of what is known about its behaviour was inferred from numerical simulations. Maximum speeds occur at the northernmost and southernmost limits of Samborombón Bay whereas in its interior they are weaker (Figure 4 lower left panel). This last region displays a rotational feature, but at the upper and central estuary tidal currents tend to be more unidirectional; this last is also the case along the Uruguayan coast (Simionato *et al.,* 2004a). The tidal ellipses have a clockwise rotation and a west-northwest to east-southeast orientation in the southern coast, and are elongated, with an east-west orientation and a counter clockwise rotation in the northern coast (Figure 4 lower left panel). The speed of the tidal currents range between 0.2 and 0.4 $ms^{-1}$ at the salinity frontal zone (Simionato *et al*., 2006a).

Luz Clara Tejedor *et al.* (2014) studied the influence of the large inter-annual changes in the continental discharge related to the ENSO cycles on the tidal amplitude and phase. The authors showed that significant non linear interactions occur, with an increase (reduction) of the runoff accompanied by increments (reductions) of the dominant tidal constituent $M_2$ phase and reductions (increments) of its amplitude. This is a consequence of the deformation that occurs because of the interaction between the tide and the currents.

### 2.4. Winds

Winds are the main forcing of the RdP Estuary circulation, particularly in its exterior area and, as it will be discussed later, it affects estuarine circulation on every time scale. The atmospheric general circulation in the RdP region is controlled by the influence of the semi-permanent South Atlantic high pressure system. The counter-clockwise circulation associated with this centre advects warm and moist air from subtropical regions over the estuary (Minetti and Vargas, 1990). On the other hand, cold atmospheric systems coming from the south drive cold air masses over the area with a dominant periodicity of around 4 days (Vera *et al.,* 2002). The passage of these cold fronts is in occasions associated with convective storms which are usually referred as 'Pamperos'. As a result of those features, an alternation of winds from the northeast to the southwest in a scale of a few days is the dominant characteristic of wind variability in the area (illustrated in Figure 5, from Simionato *et al*., 2008). It is modulated in intra-seasonal time scales by an alternating pattern of variability which is associated with precipitation variability and northeast to southwest changes in surface winds (Nogués-Paegle and Mo, 1997; Liebmann *et al.,* 2004).

Additionally, the RdP is located in one of the most cyclogenetic regions of the Southern Hemisphere (Gan and Rao, 1991), due to waves that move along subtropical latitudes of the South Pacific and South American regions -exhibiting maximum variability in periods of 10 to 12 days- that interact with subtropical air masses over north-eastern Argentina, Uruguay and southern Brazil (Vera *et al.,* 2002). Approximately 8 cyclones per year occur; when they develop over Uruguay, they can originate very strong south-easterly winds, with speeds that exceed 15 $ms^{-1}$ (Seluchi, 1995; Seluchi and Saulo, 1996). These storms, known as 'Sudestadas' produce storms surges and floods in the upper estuary (D'Onofrio *et al.,* 1999; Santoro *et al.,* 2013; Dinápoli *et al.,* 2017), but they can be also produced by other meteorological conditions driving to strong and/or persistent winds from the east and southeast (Escobar *et al*., 2004). Sudestadas have a frequency of occurrence of around 2 to 3 events per year (Escobar *et al.,* 2004).

An onshore to offshore alternation characterizes the seasonal variations of the surface winds from summer to winter, associated to a larger frequency of north-easterlies in summer and a larger frequency of westerlies in winter (Simionato *et al.,* 2005a; Guerrero *et al.,* 1997a,b).

A linear trend analysis over the last 40 years of 20th Century showed a displacement of the summer-winter seasonal features to earlier months (Simionato *et al.,* 2005a). On inter-annual time-scales, the first leading pattern of variability describes east-west changes of surface winds (Simionato *et al.,* 2005a) that seems to be forced by the semi-biennial tropospheric oscillation excited in the western tropical Pacific (Mo, 2000); the conditions over the RdP are influenced by such oscillation through an atmospheric Rossby wave train propagating out of the tropics (Simionato *et al.,* 2005a). The second leading mode of variability is associated with anticyclonic/cyclonic wind rotations off the estuary on inter-annual time scales which are related with changes in both atmospheric and oceanic surface conditions at Southern Hemisphere high-latitudes (Simionato *et al.,* 2005a). Piola *et al.* (2005) and Meccia *et al.* (2009) suggested that variability at the ENSO frequencies in the RdP would not only be associated with runoff anomalies but also with surface wind anomalies over the estuary, which have a dominant westward (eastward) component during El Niño (La Niña) phase. The 850 hPa geopotential anomalies associated to the ENSO phases shown by Grimm *et al.* (2000) are consistent with those results. Those wind anomalies might be responsible for the relatively low extension of the RdP fresh plume to the north along the Brazilian coast, which is observed even under very high runoff conditions (Piola *et al.,* 2005).

### 2.5. Wind waves

Considering the general orientation of the RdP (from northwest to southeast) and its shallowness, only the waves propagating from the southeast can reach the upper RdP

Meteorologica

(Dragani and Romero, 2004). In general, the waves with relatively long period coming from the deep water of the Atlantic Ocean suffer refraction, shoaling and friction effects as they propagate to the interior of the estuary, that diminish wave heights by 94.9% (Dragani and Romero, 2004). Therefore, it is considered that local generation is the main cause of waves in the upper estuary (Halcrow and Partners, 1969; Dragani and Romero, 2004). Observations gathered in the area of Costanera Sur of Buenos Aires (Molinari and Castellano, 1990) showed that the most frequent periods are between 3 and 4 seconds, being unlikely those of more than 7 seconds. These results are consistent with those derived by EIH (1985). The most frequent range of significant heights are between 0.20 and 0.60 m, being unlikely waves higher than 1,50 m. At the exterior RdP, Dragani and Romero (2004) showed that the wave climate is a combination of "swell" (waves not related to local winds) and "sea" (waves generated by local winds), with dominant heights between 0.5 and 1.5 m and periods from 4 to 6 s for sea and 10 to 12 s for swell. The highest waves are more often associated with the presence of cyclones located either on the continental shelf (northern 40° S) or on the Uruguayan and southern Brazilian region (Dragani *et al*., 2013).

Dragani *et al*. (2010) reported a possible increase in wind wave heights in the south-western South American continental shelf between 32° S and 40° S during the last decades, that suggest that could be related to a shift of the semi-permanent anticyclone. This change could be associated, in turn, with the increased erosion observed in the outer estuary (Codignotto *et al*., 2012).

## 3. Mean salinity, temperature and density patterns and their seasonal cycle

Density in the RdP is controlled by salinity, whereas the changes in temperature, even though important from one to other season, only show small horizontal gradients (see discussion below). The stratification is controlled by the confluence of fresh waters from the tributary rivers over the denser waters from the Continental Shelf (Figure 6, adapted from Guerrero *et al*., 2010), which enter into the system as a topographically controlled salt wedge (Figure 7, from Guerrero *et al.,* 1997b) with an extension of between 100 and 250 km (Guerrero *et al.,* 1997a,b). This wedge determines the occurrence of a bottom saline front (see discussion below), associated with a zone of maximum turbidity (*e.g.*, Framiñan and Brown, 1996; Moreira *et al.,* 2013; Dogliotti *et al*., 2016). The location of the wedge is strongly anchored to the Barra del Indio shoal, but presents some mobility with the runoff, the tides and the winds (Meccia, 2008; Meccia *et al.,* 2013; Moreira *et al.,* 2013; Dogliotti *et al.*, 2016).

The seasonal cycle of temperature and salinity in the RdP was first reported by Guerrero *et al.* (1997a) using 1600 hydrographic stations gathered during 29 years (from 1966 to 1995). Since then, many more observations were collected, but the pattern described by those authors has not qualitatively changed (see, for instance, FREPLATA, 2005; Lucas *et al*., 2005; Guerrero *et al.*, 2010). They defined a warm period from December to March (summer in the SH), whereas the period from June to September characterizes the cold season (winter in the SH). During summer (Figure 6 upper panels), a marked gradient along the estuary axis is observed, with temperatures decreasing offshore. The bottom gradient is more abrupt than the surface one. During the cold season the distribution is more homogeneous, with similar temperatures (11 to 12 ºC) over the intermediate and exterior RdP, and in both the upper and bottom layers.

The lower panels of Figure 6 (adapted from Guerrero et al, 2010), shows the horizontal distribution of salinity at the surface (right panels) and near the bottom (left panels) for the warm and cold seasons, respectively. A similar distribution is observed near the bottom during both seasons, with a gradient along the estuary axis and high values in the maritime zone, decreasing to the inner RdP. The main differences from one to other season occur at the surface layer. During the cold season the freshwater plume of the RdP moves to the north along the Uruguay coast reaching southern Brazil (Möller et al., 2008; Piola et al., 2008), whereas during the warm season the freshwaters displaces to the south reaching Cabo San Antonio. Wind anomalies have been considered responsible for the movement and the extension of the RdP fresh plume because of the seasonal variation of the surface winds from summer to winter (Guerrero et al., 1997a,b; Simionato et al., 2001; Lucas et al., 2005; Simionato et al., 2007), with a larger frequency of north-easterlies in spring-summer and a larger frequency of south-westerlies in fall-winter (Simionato et al., 2005a).

SST variability on seasonal time scale and its relation to wind variability was explored by Simionato *et al.* (2010) using satellite SST and sea surface winds. They found that the seasonal cycle can be explained in terms of two modes. The first one, characterizing fall-early winter/spring-early summer, is related to the radiative cycle. The second one, corresponding to late summer and winter, displays warm/cold anomalies along the Uruguayan coast forced by the prevailing winds during those seasons. The SST seasonal cycle over the estuary is uncoupled from that on the open ocean, and the maxima and minima occur sooner. This is because the upper and intermediate RdP are very shallow and rapidly respond to radiation, and the reason why the thermal amplitude of the Argentinean Shelf maximizes at the upper estuary.

## 4. Circulation patterns

### 4.1.The barotropic circulation and its effects on sea level

#### 4.1.1. Circulation forced by the runoff and the winds

The barotropic (or vertically averaged) component of the flow dominates the variability of the SSH and has a strong impact on the net mass transport. For the RdP, it has been studied by means of numerical simulations (Jaime and Menendez, 1999; Simionato *et al.,* 2004b, 2006b; Piedra-Cueva and Fossati, 2007; Fossati and Piedra-Cueva, 2008; Meccia *et al.,* 2009) and from direct currents observations (Simionato *et al.,* 2006a). Their main features, as they can be summarized from those works, are discussed in what follows.

The barotropic subtidal flow (figures 8 and 9) is highly influenced by the geometry and bathymetry, the rotation of the Earth and, specially, the winds (Simionato *et al.,* 2004b). In the upper estuary, after the discharge of the tributaries, the flow concentrates along the deep North and Intermediate channels (Jaime and Menendez, 1999; Simionato *et al.,* 2004b; Piedra-Cueva and Fossati, 2007; Fossati and Piedra-Cueva, 2008). As the freshwater reaches the central part of the estuary, the effect of the rotation of the Earth (Coriolis effect) becomes to play a role and the transport concentrates to the north. Even though the RdP is shallow, the (barotropic) Rossby radius of deformation is of only 100 km (Simionato *et al.,* 2004b). Even though the Arquimedes and English banks divide the flow into two branches in the exterior part of the estuary, in the absence of winds (Figure 8, left panel) they meet again after flowing through this region. Despite the fact that the transport increases (reduces) for higher (lower) runoff conditions, the described pattern is preserved (Simionato *et al.,* 2004b)

The estuary's spatial patterns of circulation in response to wind variability are determined by wind direction more than by wind speed (Simionato *et al*., 2004b) and develop rapidly, occurring in a scale of between 3 and 9 hours (Simionato *et al.*, 2006a). Both observations (Simionato *et al.,* 2006a) and models (Simionato *et al.,* 2004b) indicate that the barotropic wind driven circulation of the estuary can be explained in terms of two modes (or characteristic spatial structures) of circulation associated to winds with either a cross-estuary or an along-estuary dominant component. This way, the estuary circulation can be sketched in terms of four patterns associated to each of the positive and negative phases of the modes (Figure 9, from Simionato *et al*., 2004b). The patterns corresponding to the first mode (Figures 9 *a*, *b* and *e*, *f*) are related to an inflow/outflow of water at the exterior part of the estuary, whereas the second mode (Figures 9 *c*, *d* and *g*, *h*) dominates when the wind blows along the estuary axis, that is, from the SE or from the NW (Simionato *et al*., 2004b, 2006a). The first mode accounts for the seasonal signal observed, for example, in the salinity field (Figure 6 right panel) and the second has a very distinctive pattern of significant SSH increase or reduction at the upper part of the estuary, respectively (Simionato *et al*., 2004b, 2006a). This last mode accounts for two extreme situations often observed at the RdP (Simionato *et al*., 2004b): the Sudestada, causing floods, and the persistent north-westward wind, causing low levels that in occasions collapse the fresh water supply to Buenos Aires city (Campetella *et al.,* 2007).

There are three different zones of the RdP in terms of their different response to geometry, bathymetry, Earth's rotation and winds (Simionato *et al.,* 2004b). The upper part of the estuary has the lowest influence of the Earth's rotation and has essentially a fluvial regime, mostly dominated by continental runoff and bathymetry; this is because it is narrow and relatively small (Simionato *et al.*, 2004b). The circulation pattern here is relatively insensitive to changes in the mean winds, but SSH has the maximum response in this area (Figure 9, right panel). The second zone is Samborombón Bay, which particular geometry isolates it from the northern portion of the estuary; the fresh water has relatively little impact here because of the Coriolis effect. Its circulation (Figure 8, inset) is weak and from the south, as a result of tidal rectification, in absence of winds; the bathymetry induces a small anticyclonic gyre on the south and a cyclonic one on the north (Simionato *et al*., 2004b). Having a wide mouth and being very shallow, this part of the estuary is very sensitive to the wind direction. The bay has a weak and retentive circulation pattern for winds blowing from directions between the NE and E (Simionato *et al*., 2004b). As these winds prevail during the warm season, it could favours the biota, favouring the region to become an area of nursery for several coastal species during that period of the year (*e.g.,* Acha and Macchi, 2000; Berasategui *et al.,* 2004; Rodrigues, 2005; Berasategui *et al.,* 2006; Acha *et al.,*2008; Jaureguizar *et al*., 2016). The third zone, the exterior part of the estuary, has more oceanic characteristics; here the circulation is influenced by the thermohaline structure. The area is naturally sensitive to the winds with a more oceanic Ekman type response (Simionato *et al*., 2004b).

The scales of variability of the wind forced barotropic circulation were studied by Meccia *et al.* (2009) from a 40-years long numerical simulation forced by realistic winds and runoff. Inter-annual variability accounts for almost 10% of the variance. Those authors show that first mode of SSH variability on this time scale is forced by runoff and (in a lesser extent) winds changes associated with the ENSO cycles. As a result, a mean anomaly of approximately 0.25 m occur at the upper estuary. Other two modes linked to weaker SSH anomalies which are consistent with the inter-annual modes of wind variability reported by Simionato *et al.* (2005a). Those modes have periodicities at around 2.5 and 10 years and are important, particularly if they act in phase, because they can provide a background for higher surges (Meccia *et al*., 2009). In contrast with the salinity and temperature field, SSH variability on seasonal time scales accounts for a relatively small percentage of variance and it is the combination of an annual and a semi-annual signal forced by the steric heating, the winds and the runoff (Saraceno *et al.*, 2014). Approximately 90% of the SSH variance is due to wind driven variability on sub-annual time scales (Saraceno *et al.,* 2014). The most significant SSH anomalies in this band are associated with cyclogenetic events in the atmosphere, occurring either over Uruguay or over the Patagonian Shelf, whereas the strengthening or weakening of the semi-permanent South Atlantic anticyclone displays a relatively less influence (Meccia *et al.,* 2009).

#### 4.1.2. Storm surges

The RdP is often affected by positive/negative storm surges due to strong and/or persistent south-easterly/north-westerly winds, which sweep the upper and intermediate estuary. While positive surges cause severe flooding, negative surges affect navigation and drinking water supply. Those surges have been studied by D'Onofrio *et al.* (1999, 2008), Escobar *et al.* (2004), Campetella *et al.* (2007) and Dinápoli *et al.* (2017), among others.

The positive surges, known as "Sudestadas", affect, in particular, the Metropolitan Area of Buenos Aires City (MABA, Moreira *et al*., 2014). Balay (1961) defined risk water levels over the Tidal Datum of the RdP at MABA in 2.50 m for alert, 2.80 m for emergency and 3.20 m for evacuation. Since records began in 1905, the maximum water level at MABA was registered in 1940. Enhanced by strong south-easterly winds, it reached 4.44 m above the Tidal Datum, being the tidal height overcome by 3.18 m. More recently, for instance in 1989 and 1993, extreme floods were also experienced at the city. Water levels reached 4.06 m and 3.95 m above the Tidal Datum, being the storm surge maximums of 3.25 m and 2.49 m, respectively (D'Onofrio *et al.,* 1999). Even though the events are not always so extreme, they are frequent, taking place several times per year (Escobar *et al.,* 2004). It had been suggested that the flooding is mainly due to combination of tides and surge (D'Onofrio *et al.,* 1999), but recent studies show that the nonlinear interactions between the surge, the tides and the large continental discharge that characterizes this estuary are very important (Dinápoli *et al.,* 2017).

Studies on changes in the frequency, duration, and height of storm surges over the period 1905-2003 show that the decadal averages of frequency and duration for positive surges have increased in the last three decades of 20$^{th}$ century, but they have decreased for negative surges (D'Onofrio *et al*., 2008). The average decadal trends of the maximum positive and negative surges in each year, +1.46 ± 0.08 mmy$^{-1}$ and +1.02 ± 0.09 mmy$^{-1}$, respectively, compare well with the relative mean water-level rise for Buenos Aires: +1.68 ± 0.05 mmy$^{-1}$ (D'Onofrio *et al.,* 2008).

### 4.2. The baroclinic circulation and its effects on the density structure

The lack of direct observations has limited the study of the baroclinic circulation(or vertically varying) in the RdP for long time. In the frame of the UNDP/GEF FREPLATA Project (FREPLATA, 2005), 6-month long ADCP current vertical profiles were measured at two locations in the RdP (denoted as ARG and PON in Figure 1, left panel). Those data together with salinity profiles gathered at and around the same locations were analyzed by Simionato *et al.* (2005b, 2006a, 2007), Meccia (2008) and Meccia *et al.*(2013), providing a first picture of the baroclinic flow in the frontal area of the estuary. Tides only account for 25% of the variance in the frontal zone, whereas the other 75% of the kinetic energy is related to internal waves in tidal frequencies (25%, at least in summer) and wind forced three-dimensional currents (50%) (Simionato *et al.,* 2005b, 2006a, 2007). In the next subsections every of those different motions will be discussed.

#### 4.2.1. Internal waves

Internal oscillations with inertial, semidiurnal and diurnal periods were observed in the RdP salinity front over long periods of the year, accounting for as much energy as the tides (Simionato *et al.,* 2005b). Those authors show that inertial oscillations result of wind relaxation, whereas semidiurnal and diurnal oscillations seem to be forced by the tides and the sea breeze, respectively, and that wave activity is clearly affected by the stratification conditions and result weaker during the observed fall than during the summer. This could be a typical feature given that in autumn both, the number of storms destroying the thermohaline structure increases, and land/sea breeze is less frequent. This suggests a likely seasonal cycle in the diurnal wave activity in this area, given that those unfavourable conditions are even more marked during winter. Internal waves are important as they can have an effect on mixing and the resuspension and transport of the sediments. Presumably, they can also affect the marine fauna, given that the salinity front is a region of spawning for several coastal species during the warm season (Simionato *et al*., 2005b).

### 4.2.2. Wind forced baroclinic currents and their impact on the density structure

Due to the estuary shallowness, currents in the stratified part of the RdP rapidly respond to wind changes at every level with a response time from 3 to 9 hours (Simionato *et al.,* 2007). Currents vertical structure is highly dependent on wind direction and can be explained in terms of two modes (or two current vertical patterns) which structure of correlation to wind is similar to that found for the vertically averaged component (Simionato *et al*., 2004b; 2006a). For winds with a dominant component perpendicular to the estuary axis, the response is in the form of vertically decaying currents (Figure 10, left panel, from Simionato *et al.,* 2007); instead, for winds with a dominant component along the estuary axis, a marked inversion in current direction between upper and lower levels occurs (Simionato *et al.,* 2007). This is a result of the geometry and bathymetry of the RdP Estuary: for winds with a dominant component perpendicular to the estuary axis the flow is not inhibited by bathymetry, whereas for winds parallel to the estuary axis the presence of the coast at the inner estuary requires a compensation of the inflow (outflow) at upper layers by an outflow (inflow) at the lower ones, originating the observed inversion in currents (Simionato *et al*., 2007).

The occurrence of different currents vertical structures (Figure 10, left panel) for different wind directions has implications on the vertical density structure that, consistently, can be observed in *in situ* vertical salinity profiles (Figure 10, right panel), so as in numerical baroclinic models solutions (Meccia *et al.,* 2013). North-easterly (south-westerly) winds produce a change in the salinity field consistent with an extension towards the southern (northern) coast of the surface front and an enhancement of the stratification along that coast. Cross-estuary winds from the SW (NE) can cause downwelling (upwelling) between Montevideo and Punta del Este (Pimenta *et al.,* 2008; Simionato *et al.,* 2010; Meccia *et al.,* 2013), with unknown consequences on the biota (see Section 4.4). When wind blows parallel to the estuary axis, the occurrence of an inversion in currents direction between upper and lower layers either enhance or weaken the vertical salinity structure (Simionato *et al.,* 2007; Meccia *et al.,* 2013). Weakening, and eventually breakdown of stratification can only occur as a consequence of persistent and/or intense south-easterly winds (Simionato *et al.,* 2007; Meccia *et al.,* 2013). Figure 11 (from Meccia *et al*., 2013) displays composites (or averages) of historical CTD salinity observations for different wind directions. Data from cruises with NE, SE, SW and NW modal wind within 10 days of the observations were composed. The inserts present the wind, from Pontón Recalada meteorological station (close to PON, Figure 1) modal distributions for each assemblage. It is interesting to note that the above described features about the response to winds can be even observed in composites collected for different wind speeds and for diverse persistence conditions in this highly variable system. It implies that the response of the salinity field is also fast, probably taking place in only a few hours (Simionato *et al.,* 2007). This fast response was confirmed with time series of temperature and salinity data gathered at a buoy anchored in the area of the salinity front (Moreira *et al*., 2013).

As an alternation of winds from north-easterlies to south-westerlies is the dominating feature of surface wind variability in synoptic to intra-seasonal scales in the region, winds are in general favourable to the maintenance of a salt wedge in this estuary (Simionato *et al.,* 2007). Even though north-westerly winds are commonly neither strong nor persistent in the region, their effect is also an intensification of stratification. Moreover, strong south-easterly winds that can destroy the vertical structure are not frequent, but occur only a few times per year in association with Sudestada events. Therefore, the combination of the estuary geometry and the prevailing wind variability makes the system itself efficient in maintaining the salinity structure (Simionato *et al.,* 2007; Meccia *et al.,* 2013) that a number of fish species use for their reproduction and that is the base of a rich ecosystem (*e.g.* Acha *et al.*, 2008; Jaureguizar *et al.*, 2016). Moreover, the semi-permanent stratification condition in the estuary make the sediment and detritus rich surface plume an almost continuous vector of productivity toward the adjacent continental shelf and open ocean (Moreira *et al*., 2013; Guerrero *et al*., 2014); this condition is occasionally reduced when rich surface estuarine water is mixed with pour underneath salt wedge water coming from the shelf (Simionato *et al.,* 2007; Meccia *et al.,* 2013).

The fact that stratification is highly affected by short term variability indicates that the reported 'seasonal cycle' (Section 2.4) can be explained not as a result of the mean winds for that season but as a consequence that summer (winter) is characterized by a higher frequency of winds from the northeast (west-southwest) sector; actually, conditions classically though as characteristic of 'summer' or 'winter' can take place during any season with high variability (Simionato *et al.,* 2007).

#### 4.2.3. Upwelling in the northern coast of the exterior RdP

Several works have concentrated on the intermittent and strong cold SST anomalies observed in the coastal region of the RdP located between Montevideo and Punta del Este when persistent north-easterly winds blow over the area (*e.g.*, Framiñán, 2005; Pimenta *et al.,* 2008; Simionato *et al.,* 2010). As an example, Figure 12, from Simionato *et al.* (2010), show the formation and fading of a cool cell observed during February 18$^{th}$ and March 8$^{th}$, 2008 at the eastern coast of Punta del Este. Note that the temperature in the cell is several degrees lower than the temperature of the surrounding waters.

The shallowness of the area might raise doubts about the possibility of occurrence of upwelling, but the phenomenon so as the associated processes have been well documented. Pimenta *et al.* (2008) linked upwelling in the area with the winds and the stratification in the shelf and suggested that the process might have a marked seasonality. This was confirmed by Simionato *et al.* (2010). They showed that the phenomenon corresponds to the prevailing mode of SST variability on intra-seasonal time scales at the northern Argentinean-Uruguayan Continental Shelf and that it is more frequent in spring and summer, whereas in fall and winter only a few cases are observed. Nevertheless, it must be emphasised that even if upwelling around Punta del Este occurs in winter, the bottom shelf waters -Subantarctic Shelf Waters- in the region have, during this period of the year, a temperature that makes them nearly indistinguishable from estuarine water temperatures (Guerrero *et al.,* 1997a,b; Simionato *et al.,* 2010). The stratification plays a role on upwelling in this area, Pimenta *et al.* (2008) and Simionato *et al.* (2010) suggested that the continental discharge might modulate its occurrence. When continental discharge is high (low), the surface front extends (retracts) offshore (onshore) the estuary thus increasing (reducing) the stability of the column along the northern coast, what would be unfavourable (favourable) to upwelling (Simionato *et al.,* 2010). Those events have been found to be frequent and very persistent, lasting for up to almost one and a half months (Simionato *et al.,* 2010).

### 4.2.4. Gravitational circulation

A remaining question is whether gravitational circulation occurs or not in the RdP Estuary. The ADCP observations collected during the UNDP/GEF FREPLATA Project (FREPLATA, 2005) at PON and ARG stations (see locations in Figure 1) show that temporal means are different from one to other observed period, very close to zero and with standard deviations that exceed them by between five to ten times (Simionato *et al.,* 2007). The analysis of the observations could not separate a significant signal occurring for all wind directions. Evidently gravitational circulation is very small compared to the wind forced signal that dominates in this estuary. Therefore, a much larger observation period would be necessary to filter out the synoptic, intra-seasonal and seasonal wind forced variability in order to properly discriminate gravitational circulation (Simionato *et al.,* 2007).

### 4.2.5. Classification in the Geyer and MacCready scale

In order to compare the RdP with other estuaries of the world, we computed the Geyer and MacCready (2014) scales to locate it in the estuarine parameter space. This space is based on the freshwater Froude number (*Fr*) and mixing number (*M*), defined as:

$$Fr = \frac{U_R}{\sqrt{\beta g H\, s_{ocean}}} \qquad\qquad M^2 = \frac{C_D U_T^2}{\omega\, N_0 H^2}$$

where:

- $U_R$ is the current associated to the river discharge, or river volume flow, divided the cross area of the estuary;
- $\beta$ is a coefficient of saline expansion (of the order $7.7\times10^{-4}$), such that the density $\rho = \rho_0(1+\beta s)$ grows with the salinity from a reference value ($\rho_0$), for fresh water;

- $g$ is the acceleration of gravity;
- $H$ is the depth;
- $s_{ocean}$ is the ocean salinity;
- $C_D$ is the drag coefficient (with values between $1\times10^{-3}$ and $2.5\times10^{-3}$);
- $U_T$ is the tidal velocity amplitude;
- $\omega$ is the tidal frequency;
- $N_0$ is the Brunt-Väissälä frequency.

This way, $M$ is based on the ratio of the tidal timescale to the vertical mixing timescale. Estuaries with high $M$ values exhibit strong tidal nonlinearity while those with small $M$ values have a more conventional estuarine dynamics. Estuaries with intermediate mixing rates show marked transitions between these regimes at timescales of the spring-neap cycle (Geyer and MacCready, 2014).

Due to the large geographical extension of the RdP and the broad range in continental discharge that it presents, both scales show a relatively large range of possible values. $M$ varies between 0.35 and 0.7, whereas $Fr$ goes from 0.006 to 0.03. This way, the RdP is, according to this classification, a 'strongly stratified' estuary, similarly to Chesapeake Bay and Hudson River (Geyer and MacCready, 2014). For the largest observed tidal speeds, the RdP can fall in the "partially mixed" area of the estuarine parameters space, so as those two other estuaries do.

Therefore, the Río de la Plata has essentially a 'conventional estuarine dynamics' and maintains a strong stratification according to Geyer and MacCready (2014) classification. This classification does not take into account the effect of the winds. But, as we discussed in the previous sections, because of its breadth, the RdP is strongly affected by winds, which natural variability is also favourable to the maintenance of the stratification during most of the time, so as the only forcing able to break it under some specific wind direction (Simionato *et al*., 2007; Meccia *et al*., 2013).

### 4.3. The path of the freshwater masses of the main tributaries and the flushing time scales

#### 4.3.1. The path of the freshwater masses of the main tributaries

The freshwater masses of the main tributaries to the RdP along the upper and intermediate estuary have been studied by means of numerical simulations by Re and Menéndez (2004), Piedra-Cueva and Fossati (2007) and Simionato *et al.* (2009), and is sketched in Figure 13 (adapted from Simionato *et al*., 2009). Even though there are some minor discrepancies between the different simulations' results and their interpretation, there is agreement that for mean runoff conditions the waters of the major tributaries of the RdP flow through the estuary along three differenced paths. The Uruguay and Paraná Guazú-Bravo waters mainly occupy the northern (Uruguayan) coast and the central part of the channel with some mixing between them, whereas the Paraná de las Palmas waters flow along the southern (Argentinean) coast. The occurrence and pattern of the path of the freshwater masses are controlled by the runoff and geometry and bathymetry of the estuary. This way, Uruguayan coast is mostly affected by waters of the Uruguay River and Argentinean coast by waters of the Paraná de las Palmas. Even though this flow scheme has been derived from numerical simulations, it is consistent with what can be inferred from the specific conductivity and bottom sediments distribution in the estuary, so as from colour satellite images (Simionato *et al*., 2009; Moreira *et al*., 2016).

The results of the simulations of Simionato *et al.* (2009) indicate that during the most frequent storm events (Sudestadas and Pamperos), even though mixing occurs, the identity and general pattern of the freshwater masses paths are preserved. Nevertheless, during those events, due to its shallowness, Argentinean coast is significantly affected by advection and mixing. The persistence of the signal introduced by the storms depends on the location, but does not exceed one week (Simionato *et al.*, 2009).

#### 4.3.2. Flushing time scales

The simulations of Simionato *et al.*(2009) also allowed for the estimation of the flushing scales for the RdP. At its upper and upper intermediate parts flushing scales are mainly related to the runoff with scarce influence of the mean winds. Given the broad range of discharge conditions observed in the estuary, time scales can be half (twice) the corresponding to mean conditions for low (high) discharge. For mean runoff, the elapsed time to the arrival of the leading edge of the Paraná de las Palmas at Buenos Aires is of around 3 days, whereas those of the Uruguay and Paraná Guazú-Bravo are of 7 and 5 days, respectively. The elapsed time to the peak concentration of a "tracer cloud" for a typical mean runoff scenario is of around 20 days at Buenos Aires. For that condition, the flushing times of the upper and upper intermediate estuary range between 10 and 60 days (Simionato *et al.,* 2009). Compared to typical net algal growth rates of the order of 0.1 per day, the weak flushing would permit the accumulation of nutrients and algal blooms (*e.g*., Silva *et al.*, 2014).

## 5. Retention mechanisms associated to circulation in the frontal zone

Apparently favoured by retention processes, the bottom salinity front of the RdP is a spawning ground for several coastal fishes (*e.g.,* Acha *et al.,* 2008; Derisio *et al.*, 2014; Jaureguizar *et al.*, 2016) and it is known as an area where sediments and debris remain trapped (*e.g.*, Moreira *et al.,* 2013; Silva *et al.*, 2014). This estuary is shallow and essentially wind driven and, moreover, in time scales relevant to biota, estuarine circulation is wind dominated and highly variable (Simionato *et al.,* 2004b, 2006a,b, 2007). Two intriguing questions are, therefore, how this system can favour retention and what the involved mechanisms are. These questions were studied by Simionato *et al.* (2008) and Acha *et al.* (2012) applying numerical simulations in which neutral particles were released along the bottom frontal zone (following the Barra del Indio Shoal) and tracked for different wind conditions. Results suggest that retentive features should be a consequence of estuarine response to natural wind variability acting over bathymetric features. For winds from most directions, particles either remain trapped near their launching position or move north-eastward to south-westward along the Barra del Indio shoal. As alternation of winds that favour along-shoal motion is the dominant feature of wind variability in the region, a retentive scenario results from prevailing wind variability. Additionally, winds that tend to export particles with a poor chance of being restored to the front are neither frequent nor persistent. Therefore, physical forcing alone generates a retentive scenario at the intermediate part of this estuary. The physical retention mechanism is more effective for bottom than for surface launched particles (Simionato *et al.*, 2008) and for low runoff conditions than for high discharge (Acha *et al.*, 2012). Wind statistics indicate that the proposed mechanism has different implications for retention along the seasons. Spring is the most favourable season, followed by summer, when particles would have a larger propensity to reach the southern area of the estuary (Samborombón Bay). Fall and winter are increasingly less favourable (Simionato *et al.*, 2008). All these features are consistent with patterns observed in the region in organisms having different life history traits.

## 6.Acknowledgments

This work is a contribution to the ANPCyT (National Agency for Scientific and Technological Research of Argentina) PICT 2014-2672; UBACYT 20020150100118BA (Universidad de Buenos Aires) and PIDDEF 2014 N°14 (Ministerio de Defensa, Secretaría de Ciencia, Tecnología y Producción para la Defensa, Subsecretaría de Investigación, Desarrollo y Producción para la Defensa, Programa de Investigación y Desarrollo para la Defensa). The data to build figure 3 were kindly provided by J. Borús from Instituto Nacional del Agua of Argentina.

## 7. References

Acha, E.M. and Macchi, G.J., 2000. Spawning of Brazilian menhaden, Brevoortia aurea, in the Río de la Plata estuary off Argentina and Uruguay. Fishery Bulletin 98, 227-235.

Acha, E.M., Mianzan, H., Guerrero, R., Carreto, J., Giberto, D., Montoya, N. and Carignan, M., 2008. An overview of physical and ecological processes in the Rio de la Plata Estuary. Continental Shelf Research, 28, 1579-1588.

Acha, E.M., Simionato, C.G., Carozza, C. and Mianzan H., 2012. Climate induced year classes' fluctuations of white mouth croaker Micropogonias Furnieri (Pisces, Sciaenidae) in the Río de la Plata Estuary, Argentina-Uruguay. Fisheries Oceanography, 21(1), 58-77, DOI: 10.1111/j.1365-2419.2011.00609.x.

Avigliano, E., Schenone, N.F., Volpedo, A.V., Goessler, W. and Fernández Cirelli, A., 2015. Heavy metals and trace elements in muscle of Silverside (Odontesthes bonariensis) and water from different environments (Argentina): Aquatic pollution and consumption effect approach. Science of the Total Environment 506-507, 102-108.

Balay, M.A., 1961. El Río de la Plata entre la atmósfera y el mar. Publicación. H-621. Buenos Aires: Servicio de Hidrografía Naval. Armada Argentina. pp. 153.

Berasategui, A.D., Acha E.M. and Fernandez Araoz, N.C., 2004. Spatial patterns of ichthyo plankton assemblages in the Río de la Plata Estuary (Argentina-Uruguay). Estuary Coastal Shelf Science, 60, 599-610.

Berasategui, A.D., Menu Marque, S., Gómez-Erache, M., Ramírez, F.C., Mianzan, H.W. and Acha, E.M., 2006. Copepod assemblages in a highly complex hydrographic region. Estuary Coastal Shelf Science, 66, 483-492.

Borús, J. and Giacosa, J., 2014. Evaluación de caudales diarios descargados por los grandes ríos del sistema del plata al río de la plata. Dirección y Alerta Hidrológico Instituto Nacional del Agua, Ezeiza, Argentina.

Borús J., Uriburu Quirno, M. and Calvo, D., 2017. Evaluación de caudales diarios descargados 470 por los grandes ríos del Sistema del Plata al estuario del Río de la Plata, Dirección de Sistemas de Información y Alerta Hidrológico - Instituto Nacional del Agua - Ezeiza, Argentina.

Campetella, C.M., D'onofrio, E., Cerne, S.B., Fiore, M.E. and, Possia, N.E., 2007. Negative storm surges in the Port of Buenos Aires. International Journal of Climatology, 27 (8), pp. 1091-1101.

Campos, J.D., Lentini, C.A., Miller, J.L. and Piola, R.A., 1999. Inter-annual variability of the sea surface temperature in the South Brazilian Bight. Geophysical Research Letters. 26(14), 2061-2064.

Canevari, P., Blanco, D., Bucher, E., Castro, G. and Davidson, I., 1998. Los Humedales de la Argentina. Clasificación, Situación Actual, Conservación y Legislación. Publicado por Wetlands Internacional y Secretaría de Recursos Naturales y Desarrollo Sustentable de la Nación. Publicación Nº 46. Buenos Aires.

Cardini, J.C., Garea, M. and Campos, M. R., 2002. Modelación del transporte de sedimentos puestos en suspensión por actividades de dragado en el Río de la Plata, para la generación en tiempo real de pronósticos de afectación de áreas costeras. Anales del Congreso de Mecánica Computacional, Santa Fé- Paraná, Argentina, Octubre de 2002. Publicado por Mecánica Computacional, 21, 2325-2342.

Cellone, F., Carol, E. and Tosi, L., 2016. Coastal erosion and loss of wetlands in the middle Río de la Plata estuary (Argentina). Applied Geography, 76, pp. 37-48.

Codignotto, J.O., Dragani, W.C., Martin, P.B., Campos, M.I., Alonso, G., Simionato, C.G. and Medina, R.A., 2011. Erosion at the Samborombón bay and changes in wind direction, province of Buenos Aires, Argentina. Revista del Museo Argentino de Ciencias Naturales, Nueva Serie, vol. 13, no. 2, pp. 135-138.

Codignotto, J.O., Dragani, W.C., Martin, P.B., Simionato, C.G., Medina, R.A. and Alonso, G., 2012. Wind-wave climate change and increasing erosion in the outer Río de la Plata, Argentina. Continental Shelf Research, 38, pp. 110-116.

Colombo, J. C., Cappelletti, N., Barreda, A., Migoya, M.C. and Skorupka, C., 2005. Vertical fluxes and accumulation of PCBs in coastal sediments of the Río de la Plata estuary, Argentina. Chemosphere, 61(9), 1345-1357.

Colombo, J. C., Cappelletti, N., Migoya, M.C. and Speranza, E., 2007. Bioaccumulation of anthropogenic contaminants by detritivorous fish in the Río de la Plata estuary: 2-Polychlorinated biphenyls. Chemosphere, 69(8),1253-60.

Combes, V. and Matano, R.P., 2014. A two-way nested simulation of the oceanic circulation in the Southwestern Atlantic. Journal of Geophysical Research: Oceans, 119

(2), pp. 731-756.

Comisión Administradora del Río de la Plata (CARP), 1989. Estudio para la evaluación de la contaminación en el Río de la Plata, Reporte Informe Comisión Administradora del Río de la Plata, Buenos Aires, pp 137.

Depetris, P.J. and Griffin, J.J., 1968. Suspended load in the Río de la Plata drainage basin. Sedimentology, 11, 53-60.

Derisio C., Bravermana, M., Gaitán, E., Hozbora, C., Ramíreza, F., Carretoa, J., Botto, F., Gagliardini, D.A., Acha, E.M. and Mianzan, H., 2014. The turbidity front as a habitat for Acartiatonsa (Copepoda) in the Río de la Plata, Argentina-Uruguay. Journal of Sea Research Volume 85, Pages 197-204.

Dinápoli, M. G., Simionato, C.G. and Moreira, D., 2017. Model sensitivity and nonlinear interactions during extreme sea level events in a wide and fast-flowing estuary: the case of the Río de la Plata. Submitted in revision to Natural Hazards and Earth System Sciences. nhess-2016-393.

Dogliotti, A, Ruddick, K. and Guerrero, R., 2016. Seasonal and inter-annual turbidity variability in the Río de la Plata from 15 years of MODIS: El Niño dilution effect. Estuarine, Coastal and Shelf Science Volume 182, Part A, Pages 27-39.

D'Onofrio, E., Fiore, M.M.E. and Romero, S., 1999. Return periods of extreme water levels estimated for some vulnerable areas of Buenos Aires. Continental Shelf Research, 19, 1681-1693.

D'Onofrio, E.E., Fiore, M.M.E. and Pousa, J.L., 2008. Changes in the regime of storm surges at Buenos Aires, Argentina. Journal of Coastal Research, 24 (1 SUPPL. A), pp. 260-265.

Dragani, W. C. and Romero, S. I., 2004. Impact of a possible local wind change on the wave climate in the upper Río de la Plata. International Journal of Climatology, 24(9), 1149-1157.

Dragani, W.C., Martin, P.B., Simionato, C.G. and Campos, M.I., 2010. Are wind wave heights increasing in south-eastern south American continental shelf between 32°S and 40°S? Continental Shelf Research, 30 (5), pp. 481-490.

Dragani, W.C., Bibiana C., Campetella, C., Possia, E. and Campos, M.I., 2013. Synoptic patterns associated with the highest wind-waves at the mouth of the Río de la Plata estuary, In Dynamics of Atmospheres and Oceans, Volumes 61–62, Pages 1-13, ISSN 0377-0265, https://doi.org/10.1016/j.dynatmoce.2013.02.001.

EIH, 1985. Estudio de antecedentes del Canal Ingeniero Emilio Mitre, Informe Final, CEDEPORMAR.

Escobar, G., Vargas, W. and Bischoff, S., 2004. Wind tides in the Río de la Plata Estuary: Meteorological conditions. International Journal of Climatology, 24, 1159-1169.

Fossati, M. and Piedra-Cueva, I., 2008. Numerical modelling of residual flow and salinity in the Río de la Plata. Applied Mathematical Modelling, 32, 1066-1086.

Framiñan, M.B. and Brown, O.B., 1996. Study of the Río de la Plata turbidity front: I. Spatial and temporal distribution. Continental Shelf Research 16, 1259-1282.

Framiñan, M.B., Etala, M.P., Acha, E.M., Guerrero, R.A., Lasta, C.A. and Brown, O.B., 1999. Physical characteristics and processes of the Río de la Plata Estuary. In: Perillo, GM, Piccolo MC, Pino Quivira M (Eds.) Estuaries of South America: Their Morphology and Dynamics, Springer, New York, pp. 161-194.

Framiñan, M. B, 2005. On the Physics, Circulation and Exchange Processes of the Río de la Plata Estuary and the Adjacent Shelf. Doctoral Dissertation. University of Miami, Rosenstiel School of Marine and Atmospheric Science, Miami, Florida, USA, 486 pp.

FREPLATA, 2005. Análisis Diagnóstico Transfronterizo del Río de la Plata y su Frente Marítimo. Documento Técnico Proyecto 'Protección Ambiental del Río de la Plata y su Frente Marítimo: Prevención y Control de la Contaminación y Restauración de Hábitats' PNUD/GEF RLA/99/G31. Fondo para el Medioambiente Global (FMAM) and Programa de las Naciones Unidas para el Desarrollo (PNUD). Edited by Comisión Administradora del Río de la Plata and Comisión Técnica Mixta del Frente Marítimo. 311 pp.

Gan, A.P. and Rao, B.V., 1991. Surface cyclogenesis over South America. Monthly Weather Review, 119, 1293-1302.

Garcia-Rodriguez, F., Brugnoli, E., Muniz, P., Venturini, N., Burone, L., Hutton, M., Rodríguez, M., Pita, A., Kandratavicius, N., Perez, L. and Verocai, J., 2014. Warm phase ENSO events modulate the continental freshwater input and the trophic state of sediments in a large South American estuary. Marine and Freshwater Research, 65: 1-11, 2014. DOI: 10.1071/MF13077.

Geyer W. R. and MacCready, P., 2014. The Estuarine Circulation. Annual Review of Fluid Mechanics 2014 46:1, 175-197. https://doi.org/10.1146/annurev-fluid-010313-141302

Glorioso, P.D. and Flather, R.A., 1995. A barotropic model of the currents off SE South America. Journal Geophysical Research, 100, 13427-13440.

Glorioso, P.D. and Flather, R.A., 1997. The Patagonian Shelf tides. Progress Oceanography, 40, 263-283.

Gómez-Erache, M., 1999. Spatial and temporal variation in the copepod community of

Montevideo Bay, Uruguay. Proceedings of the Seventh International Conference on Copepoda (Curitiba, Brazil), pp 25-31.

Gómez-Erache, M., Sans, K., Danilo, C., and Menu Marque S., 2004. Recent data on freshwater Cyclopoid Copepoda (Cyclopoida: Cyclopidae) from Uruguay. Nauplius, 11(2), 145-148.

Grimm, A., Barros, V. and Doyle, M., 2000. Climate variability in southern South America associated with El Niño and La Niña events. Journal Climate 13:35-58.

Guerrero, R.A., Acha, E.M., Framiñan, M.B. and Lasta, C.A., 1997a. Physical oceanography of the Río de la Plata Estuary, Argentina. Continental Shelf Research 17:727-742.

Guerrero, R.A., Lasta, C.A., Acha, E.M., Mianzan, H.W. and Framiñan, M.B., 1997b. Atlas Hidrográfico del Río de la Plata. Comisión Administradora del Río de la Plata - Instituto Nacional de Investigaciones y Desarrollo Pesquero. Buenos Aires - Montevideo, pp 190. I.S.B.N. nº 950-99583-1-X.

Guerrero, R.A., Piola, A.R., Molinari, G.N., Osiroff, A.P. and Jáuregui, S.I., 2010. Climatología de temperatura y salinidad en el Río de la Plata y su Frente Marítimo. Argentina-Uruguay. Instituto Nacional de Investigación y Desarrollo Pesquero, Contribución nº 1555. Mar del Plata, ISBN. 978-987-1443-03-1.

Guerrero, R.A., Piola, A.R., Fenco, H., Matano, R.P., Combes, V., Chao, Y., James, C., Palma, E.D., Saraceno, M. and Strub, P.T., 2014. The salinity signature of the cross-shelf exchanges in the Southwestern Atlantic Ocean: Satellite observations. Journal of Geophysical Research: Oceans, 119 (11), pp. 7794-7810.

Halcrow and Partners, 1969. Estudio y proyecto del canal de vinculación entre el Puerto de

Buenos Aires y el Río Paraná de las Palmas, Informe Final, DNCPyVN.

Huret, M., Dadou, I., Dumas, F., Lazure, P. and Garçona, V., 2005. Coupling physical and biogeochemical processes in the Río de la Plata plume. Continental Shelf Research, 25 (5-6), 629-653.

Jaime, P. and Menéndez, A.N., 1999. Modelo hidrodinámico "Río de la Plata 2000", Informe INA-LHA 01-183-99, Ezeiza, Argentina, pp 163.

Jaime, P. and Menéndez, A.N., 2002. Análisis del Régimen Hidrológico de los Ríos Paraná y Uruguay. Informe INA-LHA 05-216-02. Instituto Nacional del Agua, Ezeiza, Argentina, pp 150.

Jaime, P., and Menéndez, A., 2003. Vinculación entre el Caudal del Río Paraná y el Fenómeno de El Niño. Informe INA-LHA 216-02-03. Instituto Nacional del Agua, Ezeiza, Argentina, pp 88.

Jaureguizar, A., Bava, J., Carozza, C. and Lasta, C., 2003a. Distribution of the white mouth croaker (Micropogonias Furnieri) in relation to environmental factors at the Río de la Plata Estuary, South America. Marine Ecology Progress Series. 255, 271-282.

Jaureguizar, A., Menni, R., Bremec, C., Mianzan, H. and Lasta, C., 2003b. Fish assemblage and environmental patterns in the Río de la Plata estuary. Estuarine Coastal and Shelf Science, 56 (5-6): 921-933.

Jaureguizar, A., Militelli, M. and Guerrero, R., 2008. Distribution of Micopogonias Furnieri at different maturity stages along an estuarine gradient and in relation to environmental factors. Journal of the Marine Biological Association of the United Kingdom, 88(1):175-181.

Jaureguizar, A.J., Solari, A., Cortés, F., Milessi, A.C., Militelli, M.I., Camiolo, M.D., Luz

Clara, M., and García, M., 2016. Fish diversity in the Río de la Plata and adjacent waters: an overview of environmental influences on its spatial and temporal structure. Journal of fish biology, 89 (1), pp. 569-600.

Lasta, C., 1995. La Bahía Samborombón: zona de desove y cría de peces. Tesis Doctoral. Universidad Nacional de La Plata. 304 pp.

Liebmann, B., Kiladis, G., Vera, C.S., Saulo, A.C. and Carvalho, L.M.V., 2004. Subseasonal Variations of Rainfall in South America in the Vicinity of the Low-Level Jet East of the Andes and Comparison to Those in the South Atlantic Convergence Zone. Journal of Climate 17:3829–3842.

López Laborde, J., 1987. Caracterización de los sedimentos superficiales de fondo en el Río de la Plata Exterior y Plataforma adyacente. Anales Científicos Universidad Nacional Agraria La Molina, II:33-47.

Lucas, A.J., Guerrero, R.A., Mianzán, H.W., Acha, E.M., Lasta, C.A., 2015.Coastal oceanographic regimes of the Northern Argentine Continental Shelf (34-43°S) Estuarine, Coastal and Shelf Science, 65 (3), pp. 405-420.

Luz Clara Tejedor, M., Simionato, C.G., D'Onofrio, E., Fiore, M. and Moreira, D., 2014. Variability of tidal constants in the Río de la Plata estuary associated to the natural cycles of the runoff. Estuarine, Coastal and Shelf Science, vol. 148, pp. 85-96.

Machado, I., Barreiro, M. and Calliari, D., 2013. Variability of chlorophyll-a in the Southwestern Atlantic from satellite images: Seasonal cycle and ENSO influences. Continental Shelf Research Volume 53, Pages 102-109.

Meccia, V.L., 2008. Estudios de la circulación forzada por el viento en el estuario del Río de la Plata y sus implicancias en la estratificación: resultados del análisis de datos y simulaciones numéricas. PhD Thesis, University of Buenos Aires, February 2008.

Meccia, V.L., Simionato, C.G., Fiore, M.M.E., D'Onofrio, E. and Dragani, W., 2009. Sea surface height variability in the Río de la Plata Estaury from synoptic to inter-annual scales: results of numerical simulations. Estuarine, Coastal and Shelf Science doi:10.1016/j.ecss.2009.08.024.

Meccia, V.L., Simionato, C.G. and Guerrero, R., 2013. The Río de la Plata Estuary response to wind variability in synoptic time scale: salinity fields and breakdown and reconstruction of the salt wedge structure. Journal of Coastal Research 29(1):61-77, DOI: 10.2112/JCOASTRES-D-11-00063.1.

Mechoso, C.R. and Perez-Iribarren, G., 1992. Stream flow in southeastern South America and the Southern Oscillation. Journal of Climate 5:1535–1539.

Minetti, J.L. and Vargas, W.M., 1990. Comportamiento del borde anticiclónico subtropical en Sudamérica. II Parte. Rev Geofísica 33:177- 190.

Mo, K.C., 2000. Relationships between low-frequency variability in the Southern Hemisphere and sea surface temperature anomalies. Journal of Climate 13:3599–3610.

Molinari, G. and Castellano, R.D., 1990. Estudio de la Costanera Sur de la Ciudad de Buenos Aires - Determinación de las condiciones hidrodinámicas, Informe LHA-INCYTH 059-09-90.

Möller, Jr O.O., Piola, A.R. and Freitas, A.C., 2008. The effects of river discharge and seasonal winds on the shelf off southeastern South America. Continental Shelf Research 28(13):1607-1624.

Moreira, D., Simionato, C.G., Gohin, F., Cayocca, F., and Luz Clara Tejedor, M., 2013. Suspended matters mean distribution and seasonal cycle in the Río de la Plata estuary and the adjacent shelf from MODIS and *in situ* observations. Continental Shelf

Research, 68, 51-66.

Moreira, D., Briche, E., Falco, M., Robledo, F.A., Murgida, A., Gatti, I., Duville, M., Partucci, H., Re, M., Lecertura, E., Kazimierski, L., Etala, P., Campetella, C., Ruiz, J., Vera, C., Saulo, C., Simionato, C., Saraceno, M., Luz Clara, M., D´Onofrio, E., Dragani, W., Bertolotti, M., Saucedo, M. y Vidal, R., 2014.Anticipando la Crecida. Tools for the contribution in risk and disaster management due o southeasterly winds and precipitation floods in "La Ribera" district, Buenos Aires province, Argentina. Coastal Risks: Hazards, Issues, Representations, Management, 244-251.

Moreira, D., 2016. Estudio de los procesos que determinan el transporte de los sedimentos finos y su variabilidad en el Río de la Plata en base a simulaciones numéricas y observaciones satelitales e *in situ*. Tesis Doctoral. Universidad de Buenos Aires.

Moreira, D., Simionato, C.G., Dragani, W., Cayocca, F., and Luz Clara Tejedor, M., 2016. Characterization of bottom sediments in the Río de la Plata estuary. Journal of Coastal Research, 32(6), 1473–1494. Coconut Creek (Florida), ISSN 0749-0208.

Nagy, G.J., Martinez, C.M., Caffera, R.M., Pedraloza, G., Forbes, E.A., Perdomo, A.C. and Laborde, J.L., 1997. The hydrological and climatic setting of the Río de la Plata. In: Wells PG, Daborn GR (eds) The Río de la Plata, An Environmental Overview, An Eco Plata Project Background Report. Dalhausie University, Halifax, Nova Scotia, pp 17-68.

Nogués-Paegle, J. and Mo, K.C., 1997. Alternating wet and dry conditions over South America during summer. Monthly Weather Review, 125:279-291.

O'Connor, W.P., 1991. A numerical model of tides and storm surges in the Río de la Plata estuary. Continental Shelf Research, 11:1491–1508.

Ottman, F. and Urien, C.M., 1966. Sur quelques problemes sedimentologiques dans le Río de la Plata. Revue de Géographie Physique et Géologie Dynamique 8:209-224.

Parker, G., Cavalloto, J.L., Marcolini, S. and Violante, R., 1986. Los registros acústicos en la diferenciación de sedimentos subácueos actuales (Río de la Plata). Primera Reunión de Sedimentología Argentina, pp 32-44.

Piedra-Cueva, I. and Fossati, M., 2007. Residual currents and corridor of flow in the Rio de la Plata. Applied Mathematical Modelling 31:564–577.

Pimenta, F., Garvine, R.W. and Münchow, A., 2008. Observations of coastal upwelling off Uruguay down shelf of the Plata estuary, South America. Journal of Marine Research 66:835–872.

Piola, A.R., Matano, R.P., Palma, E.D., Möller, O.O. and Campos, E.J.D., 2005. The influence of the Plata River discharge on the western South Atlantic shelf. Geophys Research Letters 32:L01603 doi:10.1029/2004GL021638.

Piola, A.R., Romero, S.I., Zajaczkovski, U., 2008. Space-Time variability of the Plata plume inferred from ocean color. Continental Shelf Research 28:1556-1567.

Re, M. and Menéndez, A., 2004. Estudio de los corredores de flujo del Río de la Plata interior a partir del modelo de circulación RPP-2D. Proyecto LHA 216 Informe LHA 04-216-04 Ezeiza, Argentina, pp 58.

Robertson, A.W. and Mechoso, C.R., 1998. Interannual and decadal cycles in river flows of Southeastern South America. Journal of Climate 11:2570–2581.

Rodrigues, K.A., 2005. Biología reproductiva de la saraquita, Ramnogasterarcuata del estuario del Río de la Plata. MS Thesis, University of Mar del Plata, Argentina, 40 pp.

Santoro, P.E., Fossati, M. and Piedra-Cueva, I., 2013. Study of the meteorological tide in the Río de la Plata. Continental Shelf Research, 60, pp. 51-63.

Saraceno, M., Simionato, C.G. and Ruiz Etcheverry, L., 2014. Sea surface height trend and variability at seasonal and interannual time scale in the southeastern south America Continental Shelf between 27°S and 40°S. Continental Shelf Research. 91, 82-94. Editada por Elsevier Science. P.O. Box 211 1000 AE Amsterdam. The Netherlands. ISSN: 0278-4343.

Sathicq, M.B., Bauer, D.E. and Gómez, N., 2015. Influence of El Niño Southern Oscillation phenomenon on coastal phytoplankton in a mixohaline ecosystem on the southeastern of South America: Río de la Plata estuary. Marine Pollution Bulletin, 98 (1-2), pp. 26-33.

Schuerch, M., Scholten, J., Carretero, S., García-Rodríguez, F., Kumbier, K., Baechtiger, M. and Liebetrau, V., 2016. The effect of long-term and decadal climate and hydrology variations on estuarine marsh dynamics: An identifying case study from the Río de la Plata. Geomorphology, 269, pp. 122-132.

Seluchi, M.E., 1995. Diagnóstico y pronóstico de situaciones sinópticas conducentes a ciclogénesis sobre el este de Sudamérica. Geofis Int 34:171-186.

Seluchi, M.E. and Saulo, A.C., 1996. Possible mechanisms yielding an explosive coastal cyclogenesis over South America: experiments using a limited area model. Australian Meteorology Magazine 47:309-320.

Shiklomanov, I. A., 1998. A summary of the Monograph World Water Resources. A new appraisal and assessment for the 21st Century. UNEP, Society and Cultural Organization.

SHN, 2017. Tablas de Marea. Buenos Aires, Argentina: Servicio de Hidrografía Naval, Ministerio de Defensa Publicación H 610.

Silva, C.P., Marti, C.L and Jörg I., 2014. Horizontal transport, mixing and retention in a large, shallow estuary: Río de la Plata. Environmental Fluid Mechanics, Vol. 14, 2014, p. 1173- 1197.

Simionato, C.G., Nuñez, M.N. and Engel, M., 2001. The salinity front of the Río de la Plata - a numerical case study for winter and summer conditions. Geophysical Research Letters 28(13), 2641-2644.

Simionato, C.G., Dragani, W.C., Nuñez, M.N. and Engel, M., 2004a. A set of 3-D nested models for tidal propagation from the Argentinean Continental Shelf to the Río de la Plata Estuary – Part I $M_2$. Journal of Coastal Research 20:893-912.

Simionato, C.G., Dragani, W.C., Meccia, V.L. and Nuñez, M.N., 2004b. A numerical study of the barotropic circulation of the Río de la Plata Estuary: sensitivity to bathymetry, Earth rotation and low frequency wind variability. Estuarine, Coastal and Shelf Science 61:261-273.

Simionato, C.G., Vera, C.S. and Siegismund, F., 2005a. Surface wind variability on seasonal and interannual scales over Río de la Plata area. Journal of Coastal Research 21:770–783.

Simionato, C.G., Meccia, V.L., Dragani, W.C. and Nuñez, M.N., 2005b. Barotropic tide and baroclinic waves observations in the Río de la Plata Estuary. Journal of Geophysical Research Oceans 110:C06008. doi:10.1029/2004JC002842.

Simionato, C.G., Meccia, V.L., Dragani, W.C., Guerrero, R.A. and Nuñez, M.N., 2006a. The Río de la Plata Estuary response to wind variability in synoptic to intra-seasonal scales: barotropic response. Journal of Geophysical Research Oceans 111:C09031 doi:10.1029/2005JC003297.

Simionato, C.G., Meccia, V.L., Dragani, W.C. and Nuñez, M.N., 2006b. On the use of the NCEP/NCAR surface winds for modeling barotropic circulation in the Río de la Plata Estuary. Estuarine, Coastal and Shelf Science 70:195-206.

Simionato, C.G., Meccia, V.L., Guerrero, R.A., Dragani, W.C. and Nuñez, M.N., 2007. The Río de la Plata Estuary response to wind variability in synoptic to intra-seasonal scales: II Currents vertical structure and its implications on the salt wedge structure. Journal of Geophysical Research Oceans 112:C07005 doi:10.1029/2006JC003815.

Simionato, C.G., Berasategui, A., Meccia, V.L., Acha, M.E. and Mianzán, H., 2008. Short time-scale wind forced variability in the Río de la Plata Estuary and its role on ichthyoplankton retention. Estuarine, Coastal and Shelf Science 76:211-226 doi:10.1016/j.ecss.2007.07.031.

Simionato, C.G., Meccia, V.L. and Dragani, W.C., 2009. On the path of plumes of the Río de la Plata Estuary main tributaries and their mixing scales. GEOACTA 34:87-116.

Simionato, C.G., Luz Clara Tejedor, M., Campetella, C., Guerrero, R. and Moreira, D., 2010. Patterns of sea surface temperature variability on seasonal to sub-annual scales at and offshore the Río de la Plata Estuary. Continental Shelf Research 30:1983-1997, doi:10.1016/j.csr.2010.09.012.

Small, C. and Nicholls, R.J., 2003. A Global Analysis of Human Settlement in Coastal Zones. Journal of Coastal Research, Vol. 19, No. 3, pp. 584-599.

Urien, C.M., 1972. Río de la Plata Estuary environments. Geological Society of America Memoirs 133:213-234.

Valle-Levinson, A., 2010. Definition and classification of estuaries. In Contemporary Issues in Estuarine Physics, ed. A Valle-Levinson, pp. 1–11. Cambridge, UK:

Cambridge Univ. Press

Vera, C.S., Vigliarolo, P.K. and Berbery, E.H., 2002. Cold season synoptic scale waves over subtropical South America. Mon Weather Rev 130:684-699.

Volpedo, A.V., Yunes, T. and Fernández Cirelli, A., 2005. El humedal mixohalino de Bahía Samborombón: conservación y perspectivas. En: Humedales Fluviales de América del Sur. Hacia un manejo sustentable. Ediciones Proteger-UICN: 89-110, 570 pp.

**Figure captions**

Figure 1: Bathymetry of the Río de la Plata Estuary (in m) and main geographical and topographical features in a 3-dimensional view (right) and a plant view with isobaths (left). Note that in the 3-d view, vertical and horizontal scales are different. The points denoted as ARG and PON show the sites where ADCP data were gathered during the FREPATA Project. Adapted from Moreira (2016) and Simionato *et al.* (2008) reprinted with permission from Elsevier.

Figure 2: Colour image collected by the Moderate Resolution Imaging Spectroradiometer on board of Terra satellite (MODIS-TERRA) in April 12$^{th}$, 2007. The image shows the Río de la Plata Estuary and its main tributaries, so as geographical references. Adapted from Visible Earth, http://visibleearth.nasa.gov.

Figure 3: Monthly mean discharge ($m^3s^{-1}$) for the Uruguay river (red), the Paraná de las Palmas River (blue), the Paraná Guazú River (green) and for the total of the three (black) for the period 1980 to 2016.

Figure 4: Tidal amplitude (m) and phase (º) for the $M_2$ tidal constituent (upper left and right panels), current ellipses ($ms^{-1}$, gray colour indicates clockwise rotation and white colour indicates anti-clockwise rotation, lower left panel) and energy dissipation by bottom friction (in $wm^{-2}$, lower right panel). The figure shows how the wave propagates upstream as a Kelvin wave and that it loses its energy by bottom friction, particularly at the tips of Samborombón Bay and along the southern coast of the estuary. Adapted from Simionato *et al.* (2004a), reproduced with permission from the Coastal Education and Research Foundation, Inc.

Figure 5: Four-daily wind vectors stick diagrams for the four seasons of an arbitrary year (in this case, 1995) from the NCEP/NCAR reanalysis at 35.2°S 54.37°W. The main

feature of wind variability in the region is their alternancy from northeast to southwest; north-easterlies are more frequent in summer and south-westerlies, in winter. Reprinted from Simionato *et al.* (2008) with permission from Elsevier.

Figure 6: Mean sea temperature (left panels) and salinity (right panels) for the warm and cold seasons for the surface (upper panel) and bottom (lower panel) layers. All the figures correspond to a normal (around the mean) continental discharge condition. The figure shows the most characteristic seasonal pattern of the salinity field in the RdP, with the freshwater mass extending offshore along the northern coast of the estuary in winter and retracting south-westward in summer. From Guerrero *et al.* (2010).

Figure 7: Vertical salinity profiles (in PSU) in the RdP along three different sections (a) north, (b) central and (c) south, for the warm (left) and the cold (right) seasons. The extension and changes in the stratification during the year can be appreciated, in particular along the northern section. From Guerrero *et al.* (1997b).

Figure 8: Model derived residual (subtidal) transport stream function (thousands of $m^3s^{-1}$) at the RdP and a detail for Samborombón Bay (inset) for a runoff of 20,000 $m^3s^{-1}$ in absence of winds. The magnitude of the transport between two isolines equals the difference between their associated values. Reprinted from Simionato *et al.* (2004b), with permission from Elsevier.

Figure 9: Main residual transport stream function (in thousands of $m^3s^{-1}$) patterns (left panel) and mean sea surface elevation (cm) patterns (right panel) at the RdP estuary related to winds blowing from different sectors. The magnitude of the transport between two isolines equals the difference between their associated values. The RdP is very sensitive to the winds and behaves as a semi-enclosed basin. For winds from the southeast/northwest the circulation induces an increment/reduction of the level at the upper estuary. For winds with a component perpendicular to the estuary axis the

circulation is characterized by changes over the northern and southern coast of the estuary. Adapted from Simionato *et al.* (2004b), reprinted with permission from Elsevier.

Figure 10: Left: Characteristic current profiles for winds blowing from different sectors as derived from ADCP data collected at ARG (see location in Figure 1). Right: Composites of salinity profiles in the vicinity of ARG for winds blowing from the NE, SE, SW and NW directions. For winds with a dominant component perpendicular to the estuary axis, the response is in the form of vertically decaying currents, whereas for winds with a dominant component along the estuary axis, a marked inversion in current direction between upper and lower levels occurs. The vertical density structure responds to currents: for north-easterly/south-westerly winds an extension towards the southern/northern coast of the surface front and an enhancement of the stratification along that coast occur; only for south-easterly wind stratification can be broken. Adapted from Simionato *et al.* (2007), reprinted with permission from Elsevier.

Figure 11: Composites of observed surface salinity fields (PSU) for winds blowing from different sectors. CTD data from oceanographic cruises and winds at Pontón Recalada station (close to PON, figure 1) were used. The insets show the wind histograms corresponding to the data composed. The response to winds can be observed in composites collected over different times of the year, indicating that it is very fast and that variability dominates in this estuary. From Meccia *et al.* (2013), reproduced with permission from the Coastal Education and Research Foundation, Inc.

Figure 12: Upwelling event observed during February $18^{th}$ and March $8^{th}$, 2008 offshore Punta del Este, observed from satellite blended SST (combination of infrared and microwave observations, contours in °C). The arrows represent the wind in $ms^{-1}$ from the NCEP-NCAR reanalyses. When the wind starts blowing from the northeast, the

development of a cold cell occurs very rapidly. The cell also rapidly decays when the wind direction changes. Reprinted from Simionato *et al.* (2010) with permission from Elsevier.

Figure 13: Schematic representation of the path of the water masses of the RdP Estuary main tributaries. The Uruguay, Paraná Guazú-Bravo and Paraná de las Palmas waters tend to flow along the northern, central and southern portions of the estuary, respectively, even though lateral mixing occurs, particularly to the northeast of the Martín García and Oyarvide islands and downstream Colonia del Sacramento, where the orientation of the coast changes. Reprinted from Simionato *et al.* (2009).

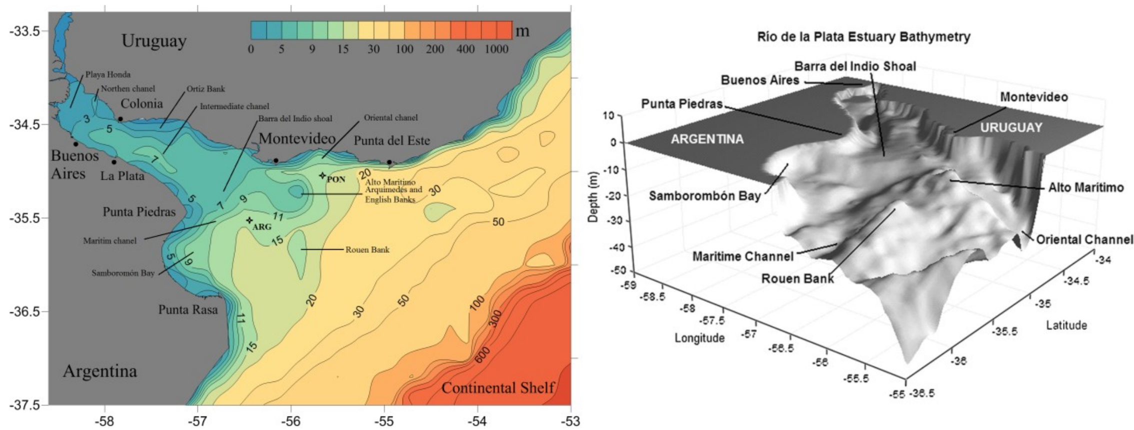
Uruguay
m
0 5 9 15 30 100 200 400 1000
Playa Honda
Northen chanel
Ortiz Bank
Intermediate chanel
Colonia
Barra del Indio shoal
Oriental chanel
Montevideo
Punta del Este
Buenos Aires
La Plata
PON
Alto Maritimo
Arquimedes and English Banks
Punta Piedras
ARG
Maritim chanel
Rouen Bank
Samboromón Bay
Punta Rasa
Argentina
Continental Shelf
-33.5
-34.5
-35.5
-36.5
-37.5
-58
-57
-56
-55
-54
-53
Rio de la Plata Estuary Bathymetry
Barra del Indio Shoal
Buenos Aires
Punta Piedras
Montevideo
ARGENTINA
URUGUAY
Samborombón Bay
Alto Marítimo
Maritime Channel
Oriental Channel
Rouen Bank
Depth (m)
Longitude
Latitude

Figure 1.

**Artículo en edición**

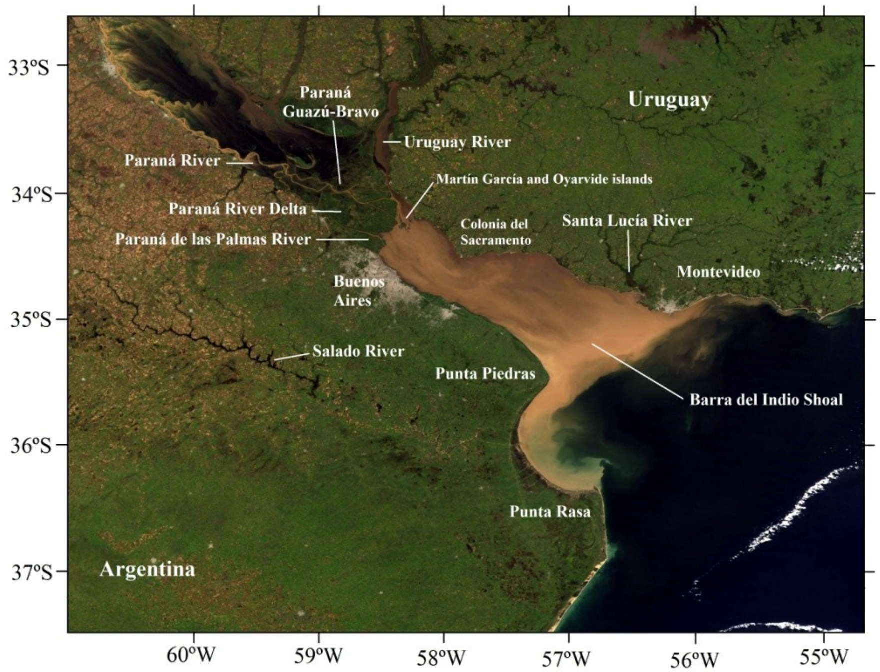


Figure 2.

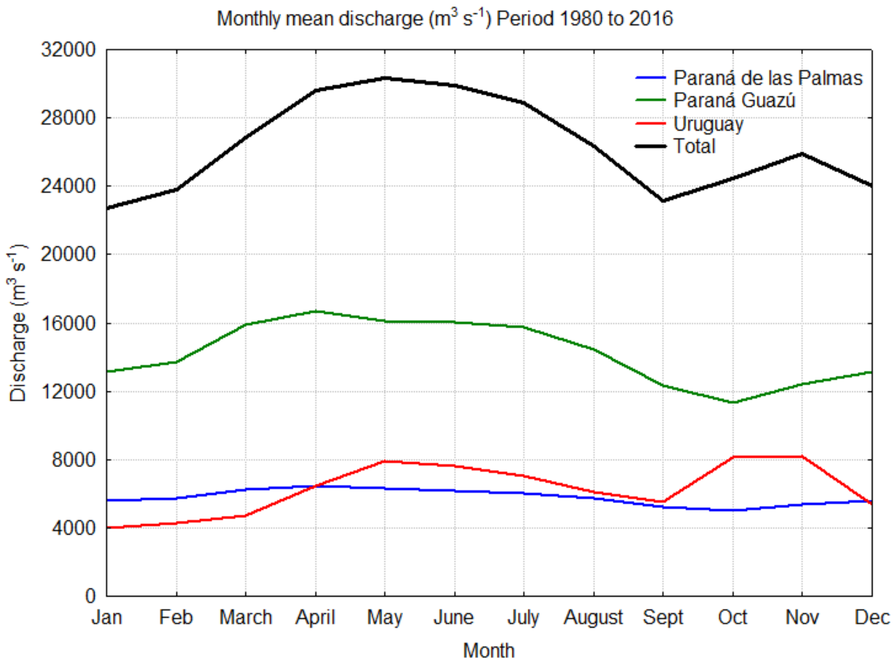
Monthly mean discharge (m3 s-1) Period 1980 to 2016
Discharge (m3 s-1)
32000
28000
24000
20000
16000
12000
8000
4000
0
Jan
Feb
March
April
May
June
July
August
Sept
Oct
Nov
Dec
Month
Paraná de las Palmas
Paraná Guazú
Uruguay
Total

Figure 3.

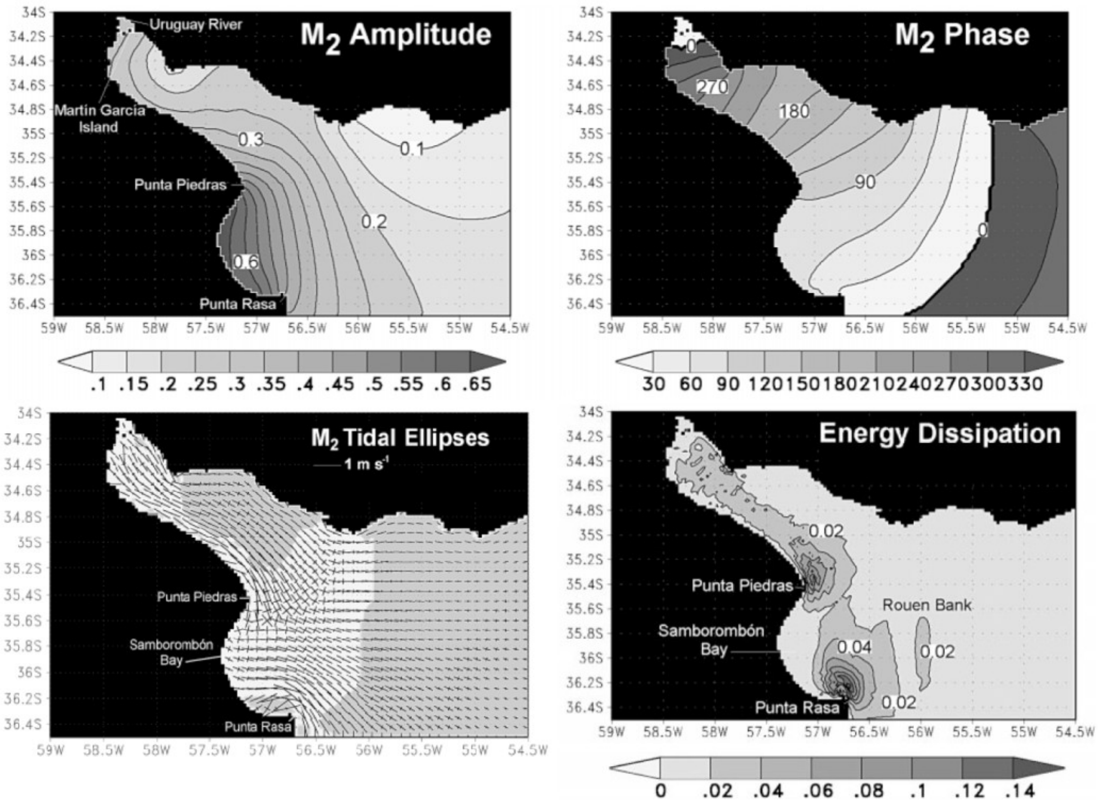
M2 Amplitude
Uruguay River
Martín García Island
Punta Piedras
Punta Rasa
0.3
0.1
0.2
0.6
.1 .15 .2 .25 .3 .35 .4 .45 .5 .55 .6 .65
M2 Phase
0
270
180
90
0
30 60 90 120 150 180 210 240 270 300 330
M2 Tidal Ellipses
1 m s-1
Punta Piedras
Samborombón Bay
Punta Rasa
Energy Dissipation
Punta Piedras
Rouen Bank
Samborombón Bay
Punta Rasa
0.02
0.04
0.02
0.02
0 .02 .04 .06 .08 .1 .12 .14
34S
34.2S
34.4S
34.6S
34.8S
35S
35.2S
35.4S
35.6S
35.8S
36S
36.2S
36.4S
59W 58.5W 58W 57.5W 57W 56.5W 56W 55.5W 55W 54.5W

Figure 4.

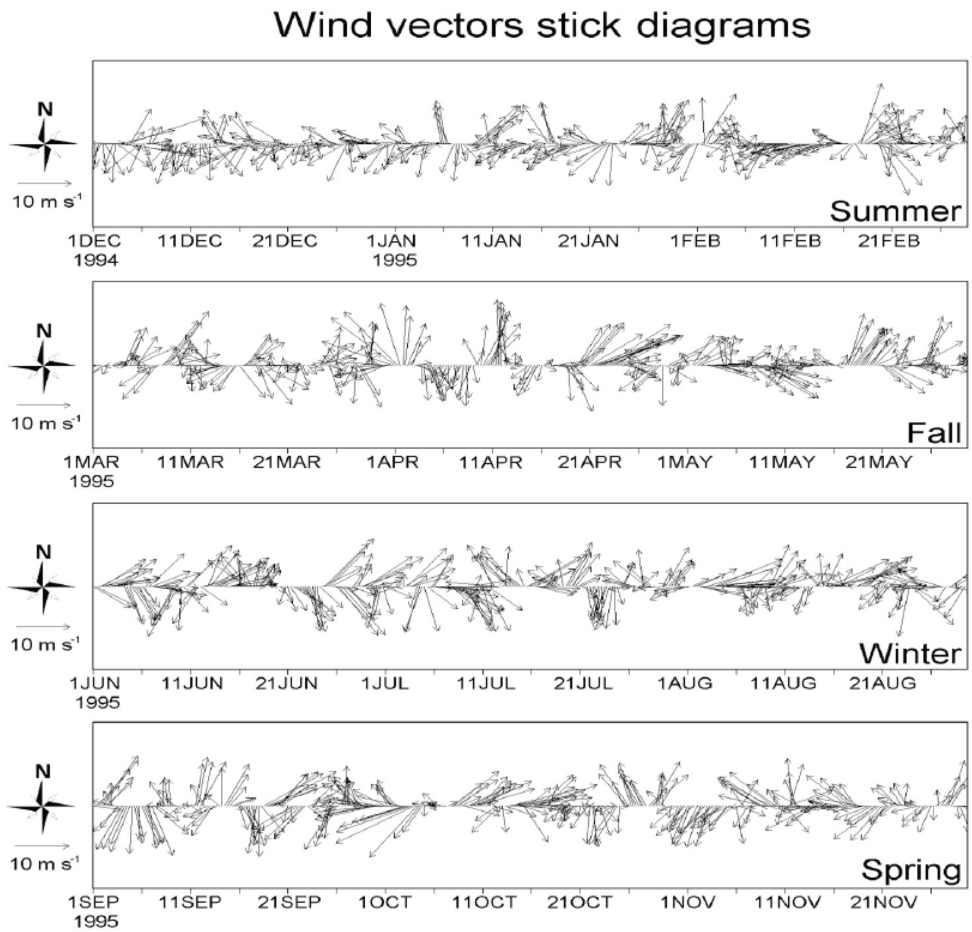
Wind vectors stick diagrams
N
10 m s-1
Summer
1DEC 1994
11DEC
21DEC
1JAN 1995
11JAN
21JAN
1FEB
11FEB
21FEB
Fall
1MAR 1995
11MAR
21MAR
1APR
11APR
21APR
1MAY
11MAY
21MAY
Winter
1JUN 1995
11JUN
21JUN
1JUL
11JUL
21JUL
1AUG
11AUG
21AUG
Spring
1SEP 1995
11SEP
21SEP
1OCT
11OCT
21OCT
1NOV
11NOV
21NOV

Figure 5.

**Artículo en edición**

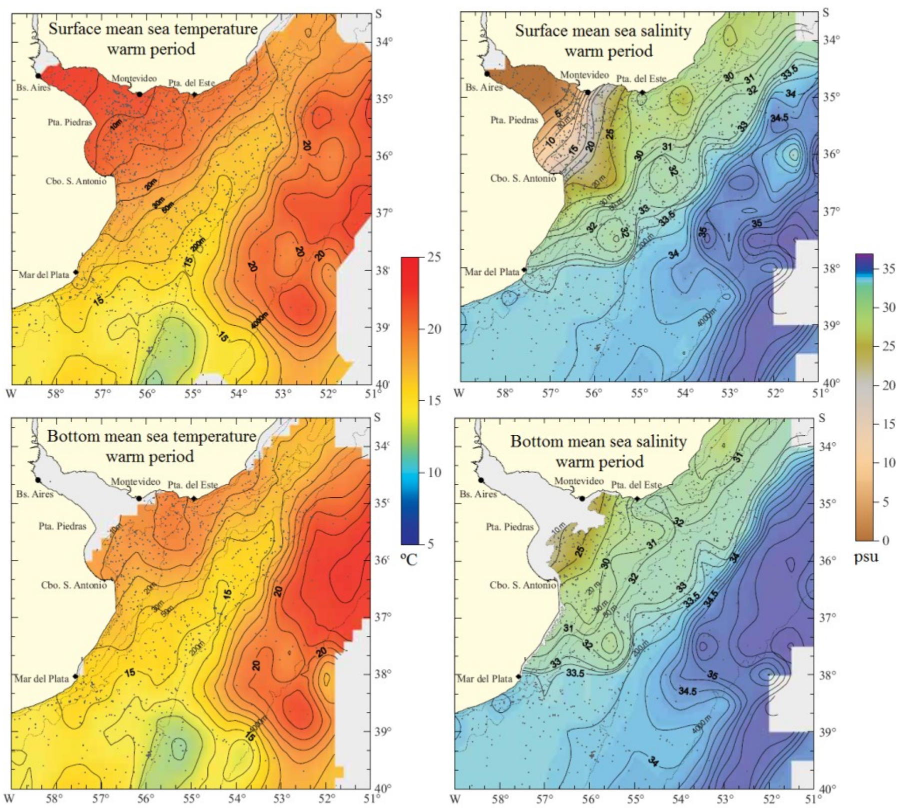

# Artículo en edición

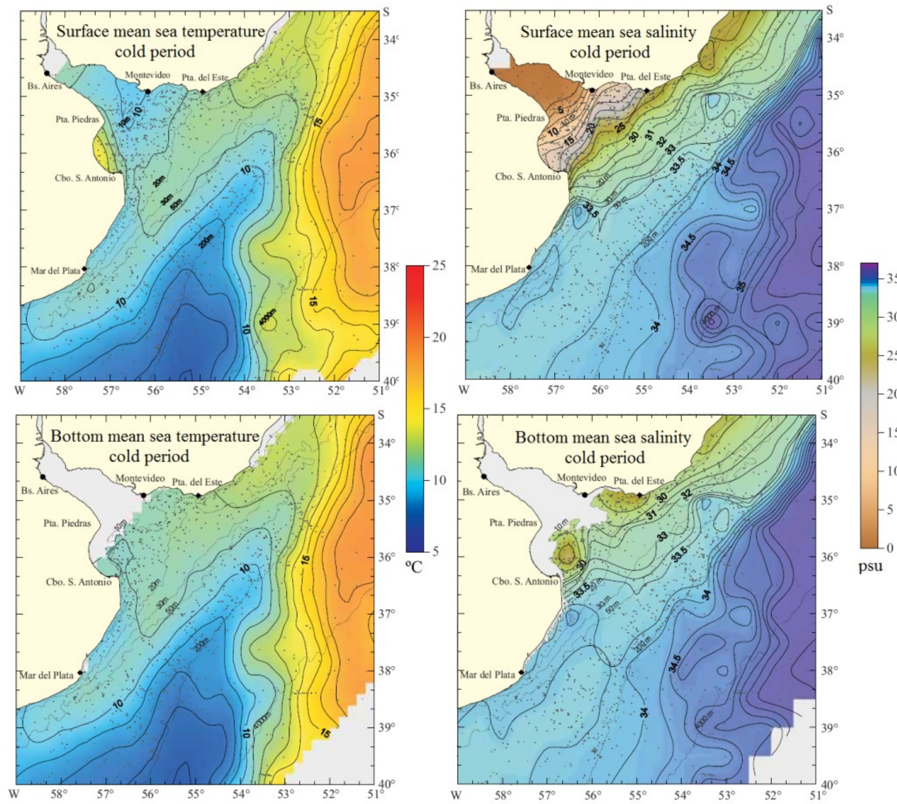


Figure 6.

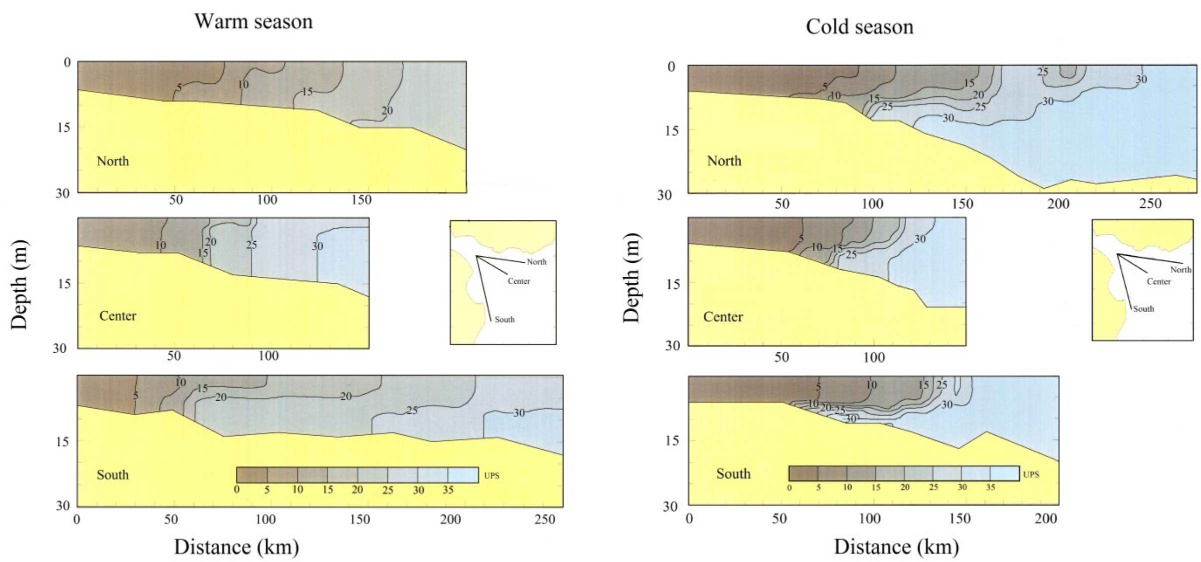
Warm season
Cold season
North
Center
South
Depth (m)
Distance (km)
UPS

Figure 7.

Barotropic (vertically averaged) circulation of the Río de la Plata

Mass transport stream function (1000 $m^3s^{-1}$)

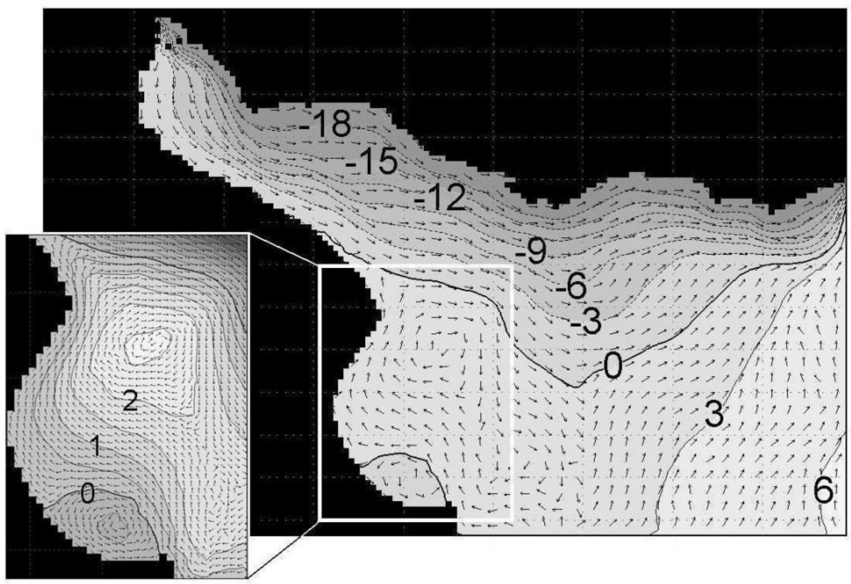


Figure 8.

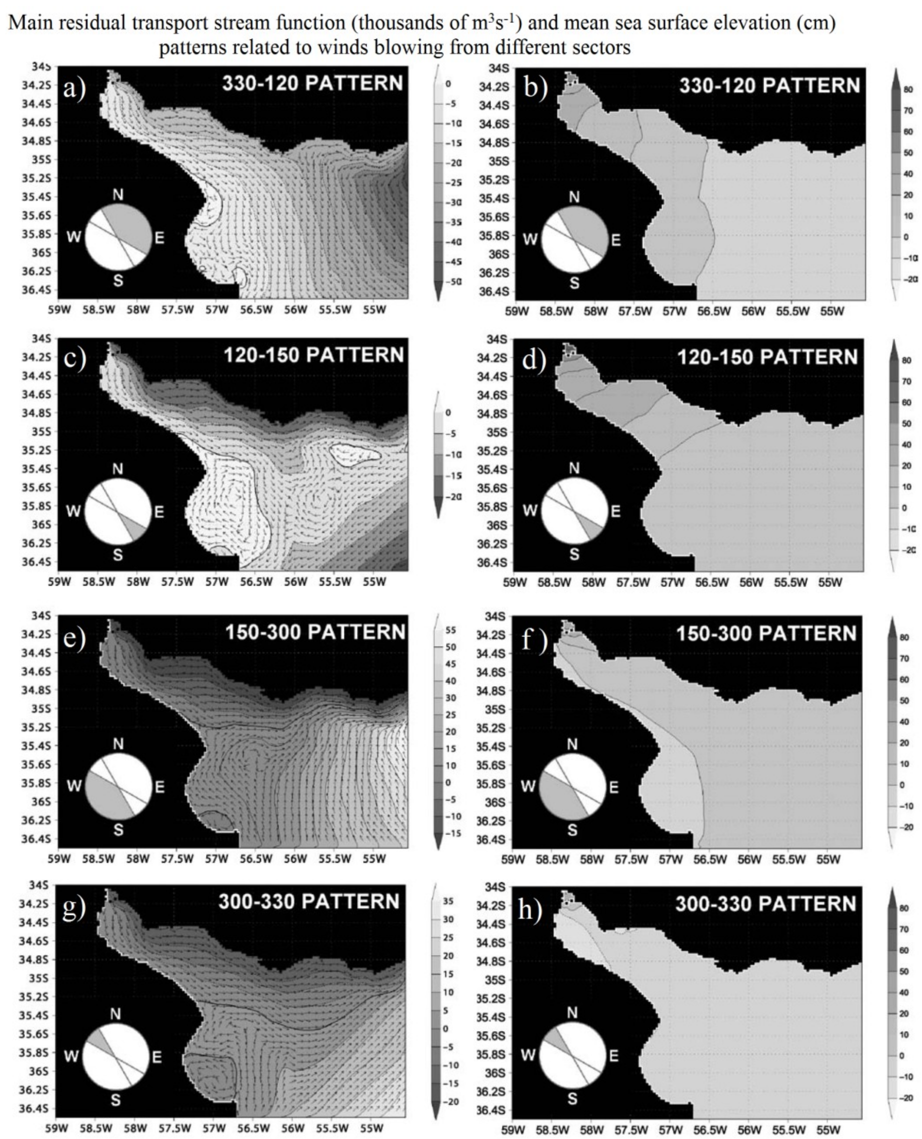

Main residual transport stream function (thousands of m³s⁻¹) and mean sea surface elevation (cm) patterns related to winds blowing from different sectors
a) 330-120 PATTERN
b) 330-120 PATTERN
c) 120-150 PATTERN
d) 120-150 PATTERN
e) 150-300 PATTERN
f) 150-300 PATTERN
g) 300-330 PATTERN
h) 300-330 PATTERN
N
S
E
W


Figure 9.

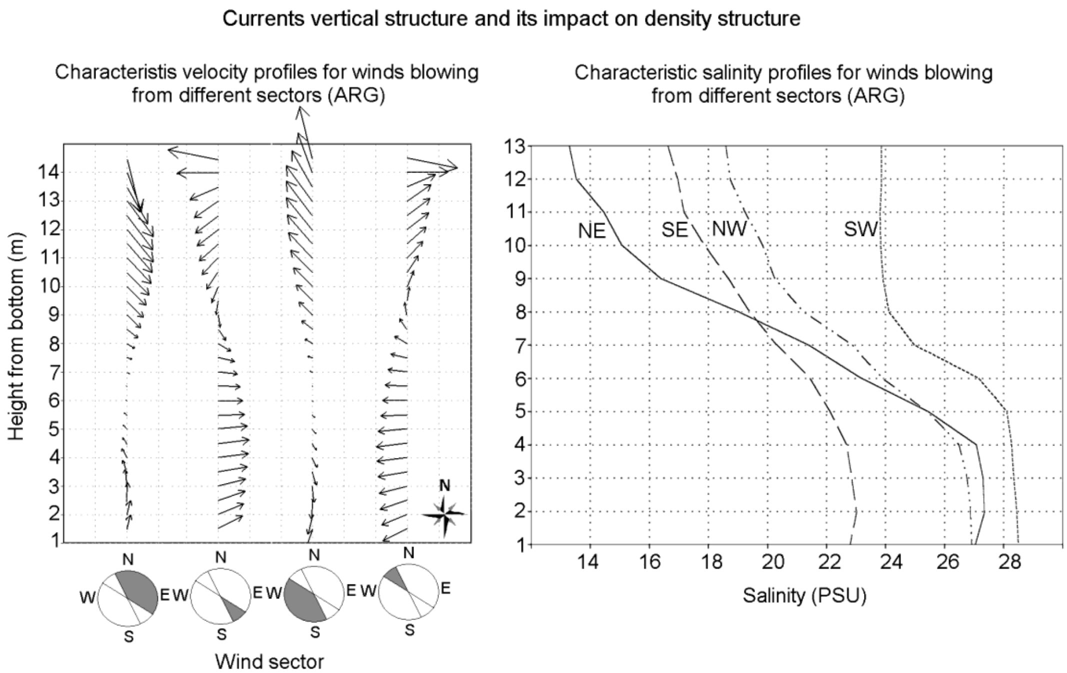
Currents vertical structure and its impact on density structure
Characteristis velocity profiles for winds blowing from different sectors (ARG)
Characteristic salinity profiles for winds blowing from different sectors (ARG)
Height from bottom (m)
Wind sector
N
S
E
W
NE
SE
NW
SW
Salinity (PSU)

Figure 10.

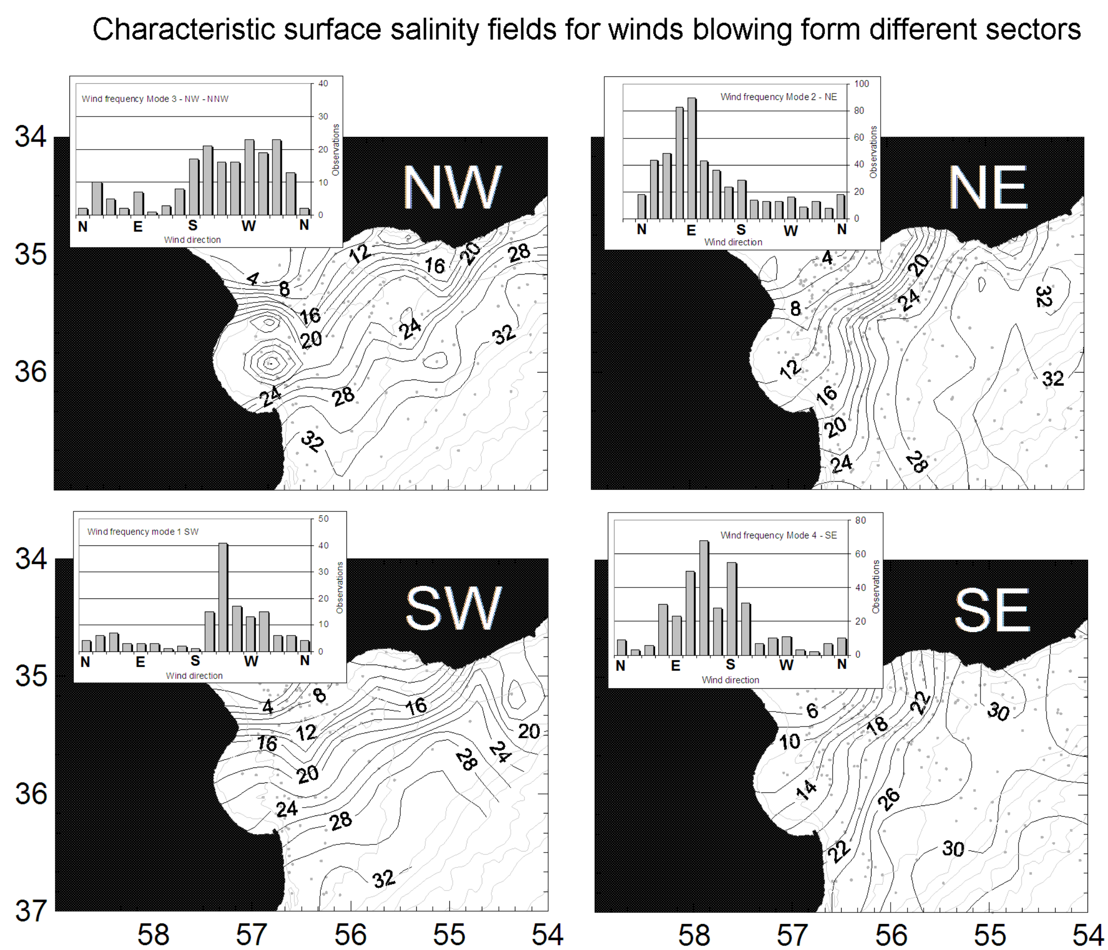
Characteristic surface salinity fields for winds blowing form different sectors
Wind frequency Mode 3 - NW - NNW
Wind frequency Mode 2 - NE
Wind frequency mode 1 SW
Wind frequency Mode 4 - SE
Wind direction
Observations
N E S W N
NW
NE
SW
SE
34
35
36
37
58
57
56
55
54

Figure 11.

Sea Surface Temperature and Wind Vectors

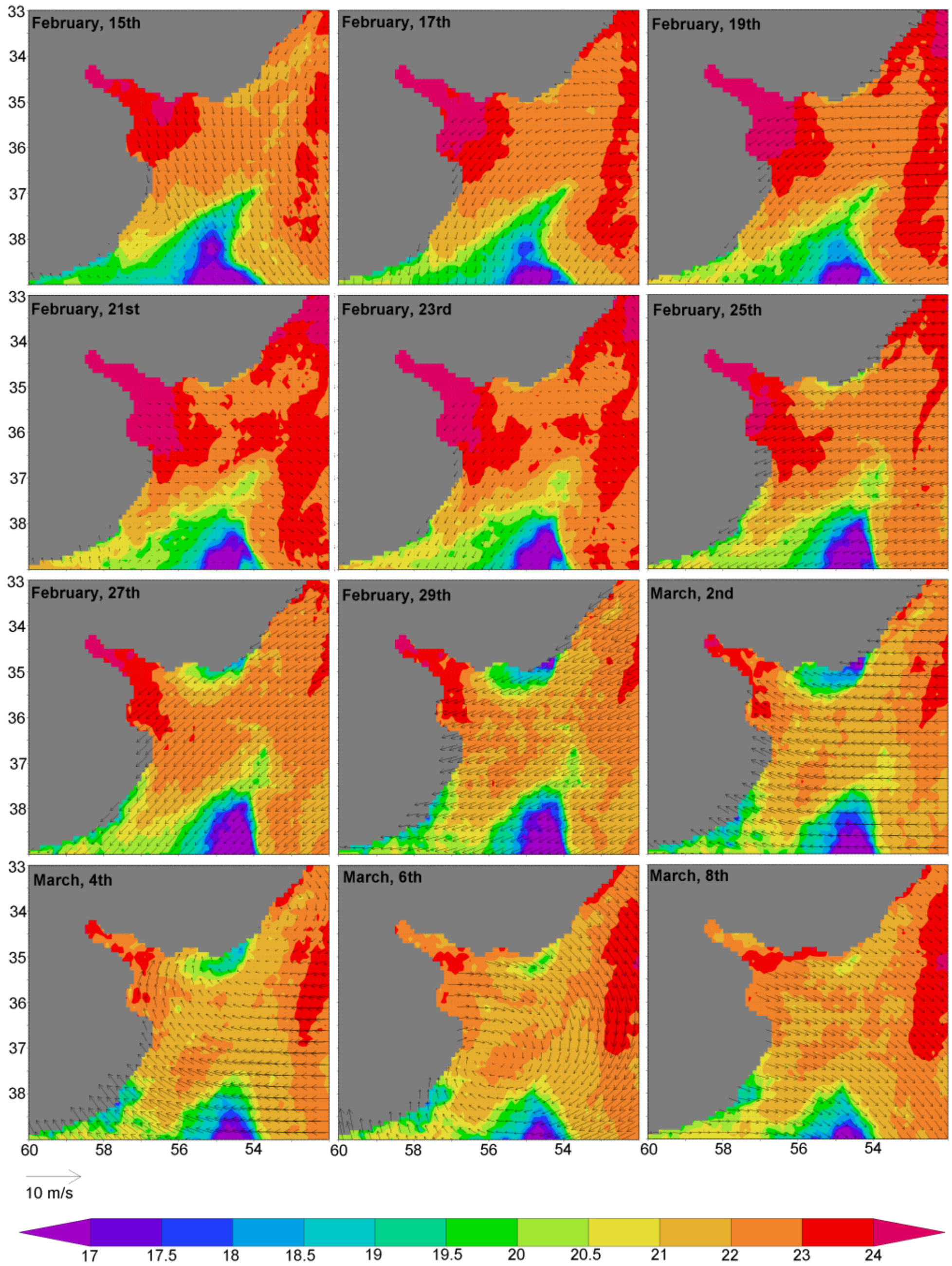


Figure 12.

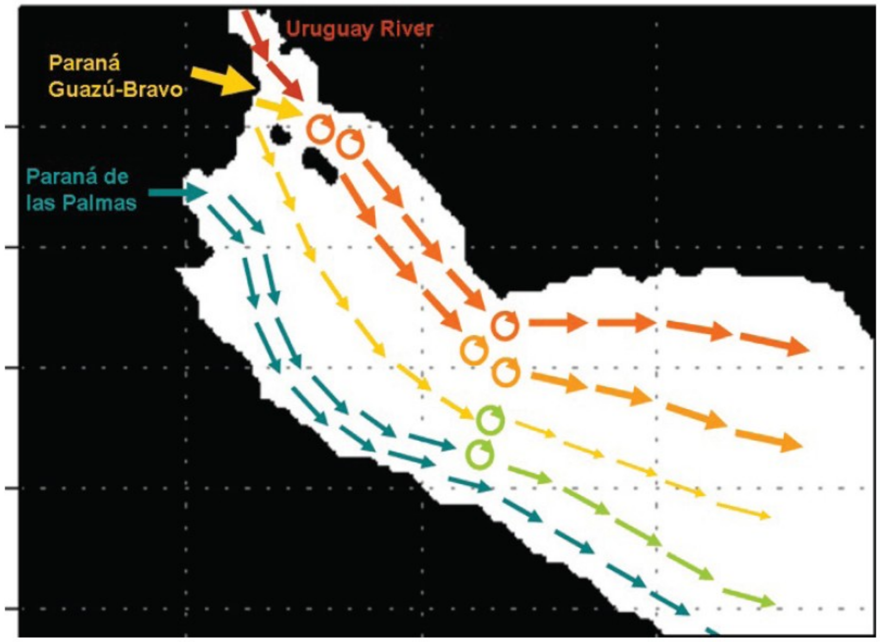


Figure 13.